inorganics

MDPI

Review

Emerging Piezoelectric Sonosensitizer for ROS-Driven Sonodynamic Cancer Therapy

Guiyun Wang [1,†], Yanxia Qi [1,†], Zhuang Liu [2,*] and Ruowei Wang [1,*]

[1] College of Nursing, Shandong Xiehe University, Jinan 250109, China; wangguiyun@sdxiehe.edu.cn (G.W.); qiyanxia@sdxiehe.edu.cn (Y.Q.)
[2] School of Materials Science and Engineering, Shandong University, Jinan 250061, China
* Correspondence: liu.zhuang@sdu.edu.cn (Z.L.); wangruowei@sdxiehe.edu.cn (R.W.)
† These authors contributed equally to this work.

Abstract: As a non-invasive modality, sonodynamic therapy (SDT) offers several advantages in cancer treatment, including deep tissue penetration and precise spatiotemporal control, resulting from the interplay between low-intensity ultrasound and sonosensitizers. Piezoelectric materials, known for their remarkable capacity of interconversion of mechanical and electrical energy, have garnered considerable attention in biomedical applications, which can serve as pivotal sonosensitizers in SDT. These materials can generate internal electric fields via ultrasound-induced mechanical deformation, which modulates the alteration of charge carriers, thereby initiating surface redox reactions to generate reactive oxygen species (ROS) and realizing the therapeutic efficacy of SDT. This review provides an in-depth exploration of piezoelectric materials utilized in SDT, with a particular emphasis on recent innovations, elucidation of underlying mechanisms, and optimization strategies for advanced biomedical piezoelectric materials. Furthermore, the incorporation of piezoelectric sonosensitizers with immunotherapy, photodynamic, chemodynamic, and chemotherapy is explored, emphasizing their potential to enhance cancer therapy outcomes. By examining the basic principles of the piezoelectric effect and its contributions to SDT, this review sheds light on the promising applications of piezoelectric materials in oncology. It also highlights future directions for improving these materials and expanding their clinical utility in tumor sonodynamic therapy.

Keywords: sonodynamic therapy; piezoelectric materials; reactive oxygen species; tumor therapy; immunotherapy

check for updates

Academic Editor: Yuui Yokota

Received: 27 January 2025
Revised: 21 February 2025
Accepted: 25 February 2025
Published: 26 February 2025

Citation: Wang, G.; Qi, Y.; Liu, Z.; Wang, R. Emerging Piezoelectric Sonosensitizer for ROS-Driven Sonodynamic Cancer Therapy. *Inorganics* **2025**, *13*, 71. https://doi.org/10.3390/inorganics13030071

Copyright: © 2025 by the authors. Licensee MDPI, Basel, Switzerland. This article is an open access article distributed under the terms and conditions of the Creative Commons Attribution (CC BY) license (https://creativecommons.org/licenses/by/4.0/).

1. Introduction

Cancer remains a tough global health challenge, with conventional therapies such as chemotherapy and radiotherapy widely utilized despite their propensity to cause severe side effects and elevate the likelihood of recurrence. Ultrasound (US) is a kind of mechanical wave with frequencies exceeding human auditory perception (>20 kHz), which has found diverse applications in clinical settings. These include diagnostic imaging, vascular thrombosis management, bone repair therapy, transdermal drug delivery, ultrasonic gene therapy, and localized drug activation [1], as shown in Figure 1a. Compared to other advanced cancer treatment modalities, such as photodynamic therapy (PDT) [2], photothermal therapy (PTT) [3], magnetothermal therapy [4], and radiotherapy [5], US has been adopted for sonodynamic therapy (SDT) to target deep-seated tumors, including pancreatic, colorectal, and liver cancers [6,7]. The reliance on magnetic fields or X-rays in magnetothermal therapy or radiotherapy often entails complex procedures and poses a substantial risk of

adverse effects, thereby limiting their clinical feasibility. In contrast, non-invasive strategies leveraging light or US are increasingly preferred for their ability to minimize collateral damage and enhance therapeutic precision. Light-based therapies leverage photosensitizers or photothermal agents to achieve antitumor effects through reactive oxygen species (ROS) production or hyperthermia, respectively [8]. Despite their potential, the limited penetration depth of light significantly restricts the efficacy of PDT and PTT [2,9]. Similar to PDT, SDT activates sonosensitizers to produce ROS via sonoluminescence, pyrolysis, or cavitation bubble collapse under ultrasonic irradiation. Additionally, SDT also generates mechanical forces such as shear stress and shock waves during acoustic cavitation, leading to direct mechanical damage to cancer cells. With its ability to penetrate deeply into tissues, effectively generate ROS, and employ diverse therapeutic mechanisms, SDT has emerged as a promising cancer treatment modality with significant clinical translation potential.

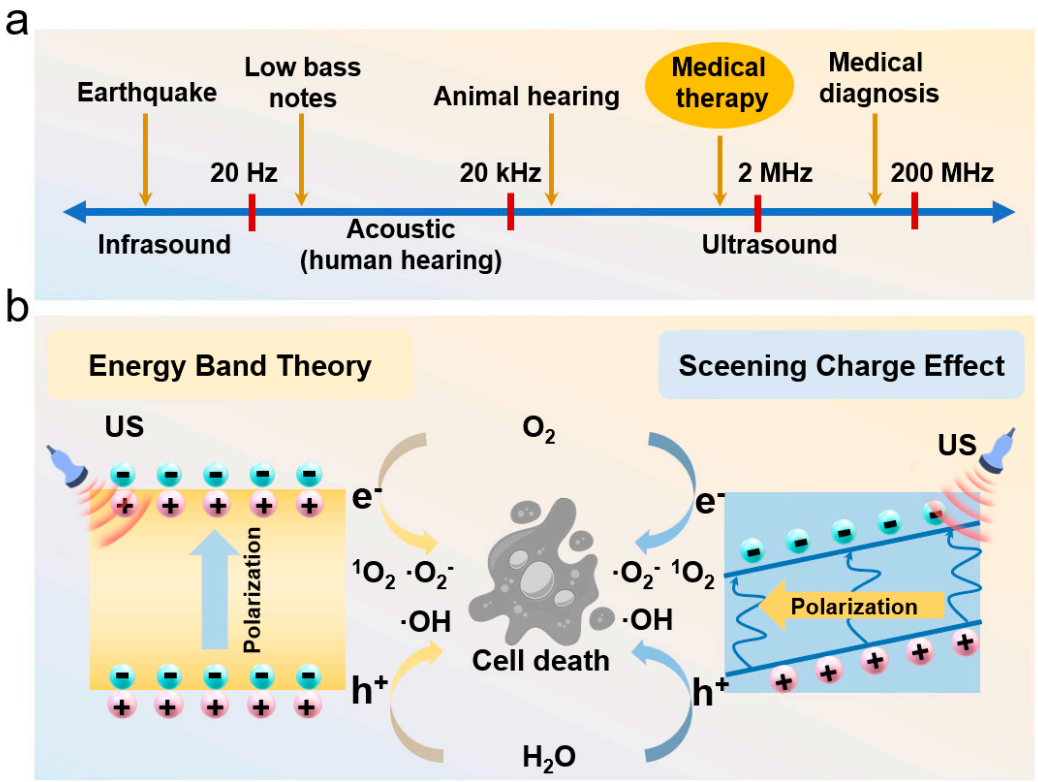


Figure 1. (**a**) Ultrasonic frequency and its application. (**b**) Schematic of two mechanisms of piezocatalysis.

Piezoelectric materials, known for their ability to interconvert mechanical and electrical energy, have demonstrated significant potential across a wide range of applications, such as actuators, sensors, ultrasonic transducers, filters, dielectric capacitors, etc. [10,11]. In the biomedical field, the piezoelectric properties of certain materials have established them as pivotal sonosensitizers in SDT, providing novel solutions for tumor treatment and various other medical challenges. Under mechanical stress, these piezoelectric materials generate internal electric fields that drive the movement of electrons (e^-) and holes (h^+) in opposing directions, thereby facilitating surface redox reactions and the production of ROS [12,13]. This phenomenon is referred to the piezocatalysis. Within a typical SDT framework, US serves as the external energy source, inducing the collapse of cavitation bubbles [14]. Beyond their catalytic roles, piezoelectric materials also play a critical part in modulating the tumor microenvironment (TME), particularly in influencing the immune landscape. ROS generation and TME remodeling can stimulate immunogenic cell death (ICD), releasing damage-associated molecular patterns (DAMPs) and tumor antigens that

activate dendritic cells (DCs) and prime cytotoxic T lymphocytes (CTLs). Recent studies have explored strategies to optimize the piezoelectric properties of materials like barium titanate ($BaTiO_3$) [15,16], zinc oxide (ZnO) [17,18], bismuth ferrite ($BiFeO_3$) [19,20], and so on. Techniques including heterojunction construction, elemental doping, and morphological tuning have further advanced these materials' capabilities in cancer treatment. While most studies have focused on inorganic piezocatalysts, it is worth noting that certain piezoelectric biocompatible polymers also possess sonodynamic potential, such as polyvinylidene fluoride (PVDF) and its copolymers (e.g., P(VDF-TrFE)), polyhydroxyalkanoates, piezoelectric peptides, and so on [21]. However, detailed discussions on these organic alternatives fall beyond the scope of this journal's primary focus.

This review provides a comprehensive analysis of the fundamental mechanisms underlying SDT using piezoelectric sonosensitizers, offering an in-depth exploration of the process. Furthermore, we examine two distinct piezocatalytic mechanisms, specifically, energy band theory and the screening charge effect, elucidating their critical roles in augmenting the efficacy of SDT (Figure 1b). The latest advancements in the application of piezoelectric materials within SDT are highlighted, with particular emphasis on prominent examples such as $BaTiO_3$, ZnO, MoS_2, and bismuth-based (Bi-based) materials. The review also delves into the burgeoning field of piezoelectric material-mediated sonodynamic immunotherapy, underscoring its potential to synergistically combine SDT with immune modulation to achieve enhanced antitumor effects. Additionally, the synergistic effects of SDT with photodynamic, chemodynamic, and chemotherapy are analyzed, showcasing its potential to enhance treatment outcomes. Considering clinical translation, the review addresses biosafety challenges, including surface modifications for stability and functionalization strategies for improved targeting. By addressing these pivotal areas, this review seeks to illuminate the current landscape and prospective trajectories of piezoelectric materials in SDT, showcasing their transformative promise in advancing cancer therapies.

2. Piezoelectric Effect: Principles and Mechanisms in SDT

2.1. Fundamentals of SDT

The remarkable ability of US to penetrate deeply into tissues while causing minimal collateral damage to surrounding healthy structures renders it highly advantageous in medical applications. For example, high-intensity focused ultrasound (HIFU) achieves tumor ablation through localized thermal effects, whereas high-intensity pulsed ultrasound enables non-thermal tissue fractionation, both serving as effective adjuncts to conventional cancer therapies [22,23]. Beyond high-intensity applications, low-intensity ultrasound has demonstrated profound non-thermal biological effects, particularly when paired with microbubbles. This combination facilitates the safe and precise delivery of therapeutics to deep-seated tissues [24,25]. An additional promising application of low-frequency US lies in its ability to activate sonosensitizers, thereby generating ROS to eradicate tumors [26]. This concept, first introduced by Umemura in the 1990s, is referred to as SDT [27]. Emerging as a derivative of PDT [9,28], SDT retains similar noninvasive tumor-fighting capabilities [26,29–31]. Compared to PDT, SDT offers significant advantages, including deeper tissue penetration and reduced phototoxicity, making it a more promising therapeutic approach.

In recent years, extensive research has explored SDT's mechanisms, yet its detailed processes remain inadequately defined due to their complexity. Proposed mechanisms are primarily tied to ultrasonic cavitation, ROS production, sonomechanical damage, and thermal effects, as shown in Figure 2 [32,33]. When ultrasonic waves (commonly 1.0–3.0 MHz at intensities of 0.5–3.0 W/cm^2) interact with sonosensitizers in liquids, they induce ultrasonic cavitation. This phenomenon arises from pressure fluctuations that create bubbles within the liquid. Cavitation is classified as either inertial or non-inertial. Inertial cavitation

involves a highly dynamic process where bubbles rapidly expand, contract, and collapse under appropriate US irradiation. The collapse generates localized sonomechanical effects, including shear forces and shock waves, as well as extreme conditions of temperature (up to 10,000 K) and pressure (approximately 81 MPa), accompanied by sonochemical reactions.

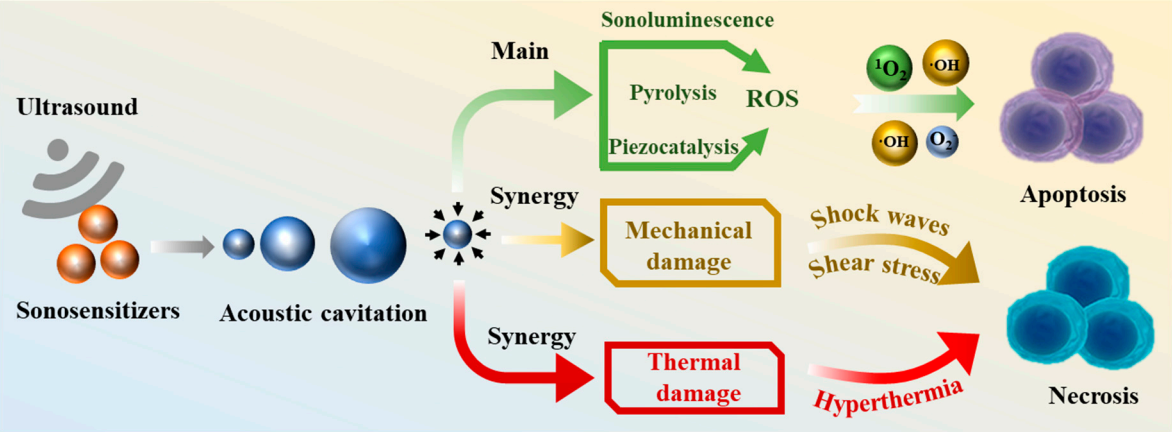


Figure 2. The schematic diagram of possible mechanisms of SDT.

Three primary mechanisms have been proposed to explain sonochemical reactions in SDT. The first, sonoluminescence, involves the emission of light during bubble collapse. This emitted light can activate energy-matched, photoactive sonosensitizers, triggering photochemical reactions similar to PDT. Sonosensitizers absorb sonoluminescent light, transitioning briefly to a singlet state before intersystem crossing to a triplet state. In this state, they interact with O_2 or biological substrates to produce free radicals or transfer energy directly to O_2, generating singlet oxygen ($^1O_2$). This process requires that the absorption spectrum of the sonosensitizers aligns with the emission spectrum of sonoluminescence [33–35]. The second proposed mechanism is pyrolysis, wherein the extreme heat and pressure during bubble collapse cause direct breakdown of sonosensitizers or their reaction with H^+ or OH^- ions formed from water thermolysis. These reactions produce free radicals, which can further react with endogenous substrates to generate secondary radicals, such as alkoxyl and peroxyl radicals [35]. Additionally, sonosensitizers, particularly piezoelectric sonosensitizers, may also be activated directly through acoustic cavitation, leading to ROS production [36]. Together, these processes contribute to ROS-mediated damage, disrupting cellular structures like the cytoskeleton and membrane, ultimately resulting in cell death. However, isolating the specific contribution of each mechanism in SDT is challenging, as outcomes depend on factors such as the type of sonosensitizer, transducer configuration, and ultrasonic parameters. Therefore, SDT should be viewed as the cumulative effect of multiple mechanisms rather than a singular ROS generation pathway.

2.2. Definition of Piezocatalysis

The development of piezoelectric materials began with the Curie brothers' discovery in 1880 of the piezoelectric properties in natural crystals, specifically single-crystal α-quartz. Around the same time, piezoelectric behavior was also identified in Rochelle salt ($NaKC_4H_4O_6{\cdot}4H_2O$). The phenomenon of electric generation induced by mechanical pressure became known as direct piezoelectricity [37]. In 1881, Gabriel Lippmann demonstrated reverse piezoelectricity, where an applied electric field caused mechanical deformation in piezoelectric materials. The underlying mechanism is rooted in the structural anisotropy of piezoelectric crystals. When subjected to external mechanical stress, atomic displacement within the unit cell disrupts the alignment between cation and anion

centers, generating a dipole moment, or polarization. The collective alignment of these dipole moments throughout the crystal results in a macroscopic piezoelectric potential (piezo-potential) [38,39]. Consequently, mechanical vibrations cause piezoelectric materials to accumulate charges of opposite polarity on their surfaces, initiating catalytic reactions, a process termed piezocatalysis [13,39]. Unlike photocatalysis, which relies on photoinduced charges, piezocatalysis depends on charges generated by mechanical force. In 2010, Hong et al. demonstrated the ability of piezoelectric materials like $BaTiO_3$ and ZnO to facilitate water splitting under ultrasound stimulation [40]. In this process, external force deforms the ZnO structure, producing a strain-induced electromotive force on its surface. This force drives charge transfer to water molecules, triggering redox reactions and breaking down H_2O into H_2 and O_2. Remarkably, this method achieved an energy conversion efficiency of up to 18%, offering an affordable and straightforward approach to water decomposition. This breakthrough laid the foundation for the concept of the piezoelectric chemical effect, later referred to as the piezocatalytic effect, in subsequent research.

3. Mechanism of Piezocatalysis

3.1. Energy Band Theory

Two primary mechanisms have been proposed to elucidate the process of piezocatalysis (Figure 1b). The first, derived from the energy band theory commonly associated with photocatalysis, posits that a piezocatalyst's ability to drive specific chemical reactions is predominantly determined by its energy band structure, including the valence band (VB) and conduction band (CB). In this context, the piezoelectric potential functions as a "gate", modulating the band configuration and facilitating the movement of charge carriers to the catalyst's surface, where they participate in the reaction. In photocatalysis, the absorption of photons excites e^- from the VB to the CB in photocatalysts, leaving behind h^+ in the VB. These photo-generated carriers initiate redox reactions based on their energy levels [41]. By contrast, in piezocatalysis, the generation of reactive carriers is not light-dependent. Instead, they are thought to originate from mechanical energy or intrinsic free charges within the material, although this mechanism remains a subject of ongoing scientific debate [42,43].

One proposed mechanism suggests that mechanical forces, such as those generated by US, can directly excite electrons from the VB to the CB. During ultrasonication, the collapse of cavitation bubbles produces extreme pressures, reaching up to 10^8 Pa at the interface between the catalyst and water, supplying sufficient energy to promote electron excitation [44–47]. Another mechanism involves indirect excitation, where mechanical energy induces vibration-driven thermal excitation. In this scenario, the collapse of cavitation bubbles creates localized "hot spots" with temperatures approaching 5000 °C near the piezocatalyst, providing the necessary thermal energy to excite electrons. Experimental validation of these theories would significantly advance understanding of piezocatalysis.

Piezoelectric modulation of band structures, utilizing intrinsic structural polarization, presents a promising approach for enhancing catalytic efficiency. When mechanical strain is applied to piezoelectric materials, a built-in piezo-potential field develops along the dipole moment within the structure, influencing the electronic states and causing band tilting. However, in contrast to perfect insulators, where band levels tilt linearly across the strained region due to the absence of mobile charges, piezoelectric semiconductors experience a different effect. Internal mobile charges within the material can orient and accumulate in response to the piezo-potential field, effectively screening the band tilting [14]. Under static deformation, this phenomenon is exacerbated as the piezo-potential drives opposing charges to continually accumulate on polar sides, creating a depolarization field that counteracts the piezoelectric polarization effect and suppresses band tilting [48]. To overcome this limitation in piezocatalysis, periodic mechanical strain, such as that induced

by ultrasonic vibration, is required. The oscillating piezo-potential prevents the stable accumulation of mobile charges, keeping them in a metastable state and maintaining the band tilting. This periodic modulation allows for the dynamic manipulation of electronic energy levels in piezoelectric semiconductors, which is crucial for catalytic activity.

This phenomenon has been validated through experimental studies, revealing several advantages of piezocatalysis. A particularly noteworthy benefit is the enhancement of redox potential. For instance, the production of radicals such as superoxide radical ($\bullet O_2^-$) and hydroxyl radical ($\bullet$OH) through water oxidation and oxygen reduction on tetragonal $BaTiO_3$ is typically thermodynamically unfavorable due to a mismatch between the band levels and the required redox potentials (Figure 3a) [49]. However, mechanical strain generates a piezo-potential of approximately 0.45 V within tetragonal $BaTiO_3$ (Figure 3c), sufficient to tilt the band structure. This realignment enables the conduction and valence band positions to align with the necessary redox potentials, facilitating radical generation through water oxidation (Figure 3b). This band rearrangement significantly enhances the catalytic performance of piezoelectric materials.

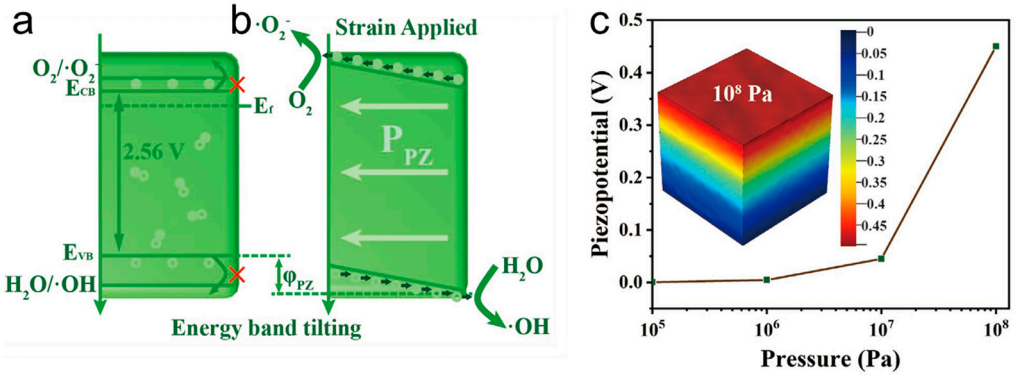


Figure 3. Illustration of $BaTiO_3$ band structure and corresponding redox potentials for ROS generation under (**a**) static conditions and (**b**) applied mechanical strain. (**c**) Simulated piezo-potential distribution within $BaTiO_3$ nanocrystals. Reproduced with permission from Ref. [49], Copyright 2020, Wiley-VCH GmBH.

3.2. Screening Charge Effect

Another mechanism, termed the screening charge effect, highlights the pivotal roles of piezo-potential and externally derived screening charges, such as surface-adsorbed charged species originating from the surrounding environment. In this framework, the piezo-potential serves as the driving force behind piezocatalysis and must satisfy or surpass the Gibbs free energy threshold of the reaction—a fundamental prerequisite for catalytic activity [12]. A key distinction between the screening charge effect and the energy band theory lies in the origin of the charges involved in redox reactions. While the energy band theory attributes reactive charges to intrinsic carriers within the material, the screening charge effect emphasizes the contribution of externally adsorbed surface charges as the primary participants in the catalytic process. Both mechanisms are versatile and applicable across various reaction types. For instance, they have been used to interpret experimental observations in common reaction systems, such as the generation of ROS through piezocatalytic oxygen reduction reactions (ORR) and water oxidation [42,50]. Despite their overlapping applicability, these two theories differ significantly in identifying the critical factors that govern the piezocatalytic process and inform the design of new catalysts. These differences highlight the need for a nuanced understanding to optimize piezocatalytic performance.

In piezoelectric materials that lack intrinsic spontaneous polarization, the particles are initially electrically neutral, with no surface compensating charges for the overlapping

of positive and negative charge centers. When mechanical strain is applied, piezoelectric polarization is induced, which draws space screening charges to the material's two polar surfaces. Once the strain decreases, the amplitude of the polarization diminishes, resulting in the subsequent release of these screening charges. This dynamic interaction of charge adsorption and release generates a current under short-circuit conditions or a potential difference under open-circuit conditions. Upon verifying the dynamic screening behavior in piezoelectric materials, the concept of the screening charge effect in piezocatalysis was introduced. By manipulating the polarization field through the piezoelectric effect, it becomes theoretically possible to precisely regulate the cycles of charge adsorption and desorption.

Based on this principle, a general mechanism using $BaTiO_3$ particles as a model for the screening charge effect has been proposed, as illustrated in Figure 4 [51]. Initially, $BaTiO_3$ remains electrically neutral because the polarization-induced bound charges are balanced by external screening charges of opposite polarity on its two polar surfaces (Figure 4a). Upon the application of compressive stress, such as that induced by ultrasonic cavitation bubbles, this equilibrium is disturbed, leading to a weakening of the polarization and the subsequent release of excess screening charges from the surface (Figure 4b). These released charges, possessing sufficient energy, can interact with substrates such as water molecules, dissolved oxygen, and H^+ or OH^- ions in the surrounding medium. This process persists until a new charge equilibrium is achieved (Figure 4c). When the applied stress is removed, the polarization recovers, generating additional bound charges. As a result, charges from the electrolyte are adsorbed back onto the surface, while charges of opposite polarity (relative to the adsorbed charges) remain in the electrolyte, contributing to further redox reactions (Figure 4d). When tensile stress is applied, the $BaTiO_3$ particles undergo a reverse cycle of screening charge adsorption and desorption, enabling similar reactions [52]. Therefore, redox reactions of piezoelectric materials are driven by cycles of polarization-mediated screening charge accumulation and release. Periodic mechanical stimulation, such as ultrasonication, cantilever oscillation, or stirring, provides a universal method to activate piezocatalysts for such processes, making this mechanism broadly applicable across various piezocatalytic systems.

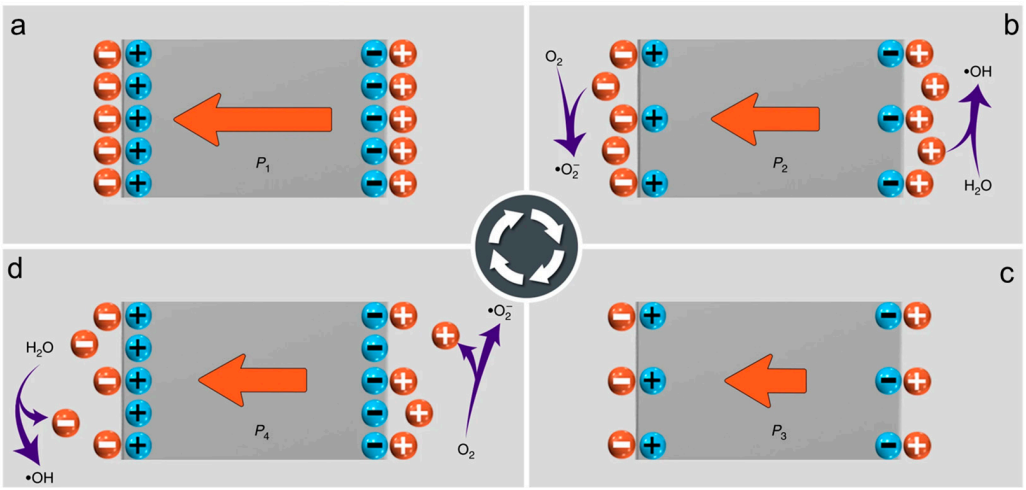


Figure 4. Working principle of piezocatalysis based on the screening charge effect. (**a**) The initial electrostatic equilibrium of $BaTiO_3$ particles. (**b**) The release of surface screening charges under compressive strain, initiating surface redox reactions. (**c**) A transient electrostatic state at maximum strain. (**d**) The adsorption of screening charges from the electrolyte upon polarization recovery, accompanied by surface reactions. Reproduced with permission from Ref. [51], Copyright 2020, Springer Nature.

4. Common Biofriendly Piezoelectric Materials for SDT

To date, numerous piezocatalysts have been developed for cancer therapy, with classic $BaTiO_3$ receiving the most extensive attention. The exploration of $BaTiO_3$ in this field began in 2019 when Shi and colleagues first incorporated noncentrosymmetric tetragonal $BaTiO_3$ (T-BTO) into cancer treatment [49]. Unlike many piezoelectric nanomaterials that exhibit complex nanostructures or consist of multiple components, $BaTiO_3$ and ZnO stand out due to their simple, well-defined compositions and structures. These materials also offer tunable morphologies, dimensions, and piezocatalytic properties, making them promising candidates for future biomedical applications [53,54]. Noncentrosymmetry, a key characteristic of effective piezocatalysts, has also been identified in certain 2D materials with stacking configurations, such as multilayer black phosphorus (BP) [55] and odd-layer molybdenum disulfide (MoS_2) [56]. This property is crucial for mechanical-to-electrical energy conversion, as it directly influences the piezoelectric coefficient (d_{33}). Generally, higher d_{33} values indicate better energy conversion efficiency, enabling more effective utilization of mechanical energy for generating electrical charges [57]. Interestingly, the d_{33} values of various piezocatalysts are comparable, highlighting their potential versatility in applications requiring piezoelectric-driven catalytic activity [58].

4.1. $BaTiO_3$

Polycrystalline BT ceramics, a classic piezoelectric material, were first developed during World War II and are often regarded as the "father of piezoceramics". In 1946, electrically poled polycrystalline BT was first demonstrated to exhibit piezoelectricity. The d_{33} of BT typically spans between 100 and 700 pC N^{-1}, with fluctuations depending on various factors such as fabrication methods, grain size, and doping agents [59]. BT has proven particularly effective in SDT, where its stable piezoelectric properties are crucial for the generation of ROS. The piezoelectric effect in BT not only causes displacement of charge centers but also facilitates charge separation and migration, thereby creating an internal electric field. This internal field drives the redox reactions crucial for ROS production (Figure 5a). Specifically, the separated electrons and holes on the BT surface promote distinct redox pathways: electrons reduce O_2 molecules to generate $\bullet O_2^-$, while holes oxidize water molecules to produce •OH. These ROS induce oxidative stress, lipid peroxidation, protein dysfunction, and DNA damage, ultimately resulting in cell death. These attributes highlight the considerable potential of BT in SDT-based tumor treatments, with its robust piezoelectric performance serving as a reliable foundation for efficient ROS generation and anticancer efficacy [36].

Constructing heterojunctions has emerged as an effective strategy to enhance the piezocatalytic efficiency of BT-based sonosensitizers. By integrating two semiconductors or materials with distinct electronic properties, heterojunctions facilitate efficient separation and transfer of electron-hole pairs, a critical factor for ROS generation in piezocatalysis. Zhao et al. developed $Cu_{2-x}O$–$BaTiO_3$ nanocubes as a piezoelectric heterostructure designed to combine SDT with chemodynamic therapy (CDT) (Figure 5b) against 4T1 breast cancer [60]. The $Cu_{2-x}O$–BTO heterojunction improved electron-hole pair separation and migration, thus amplifying ROS production for tumor destruction (Figure 5c). In 4T1 tumor bearing BALB/c mice, $Cu_{2-x}O$–BTO + US had greatly enhanced tumor inhibition, and the $Cu_{2-x}O$–BTO + US group showed the highest tumor inhibition (76%). During the therapy, all of the mice had no obvious differences in body weight change, demonstrating the high biosafety of the therapeutic modalities.

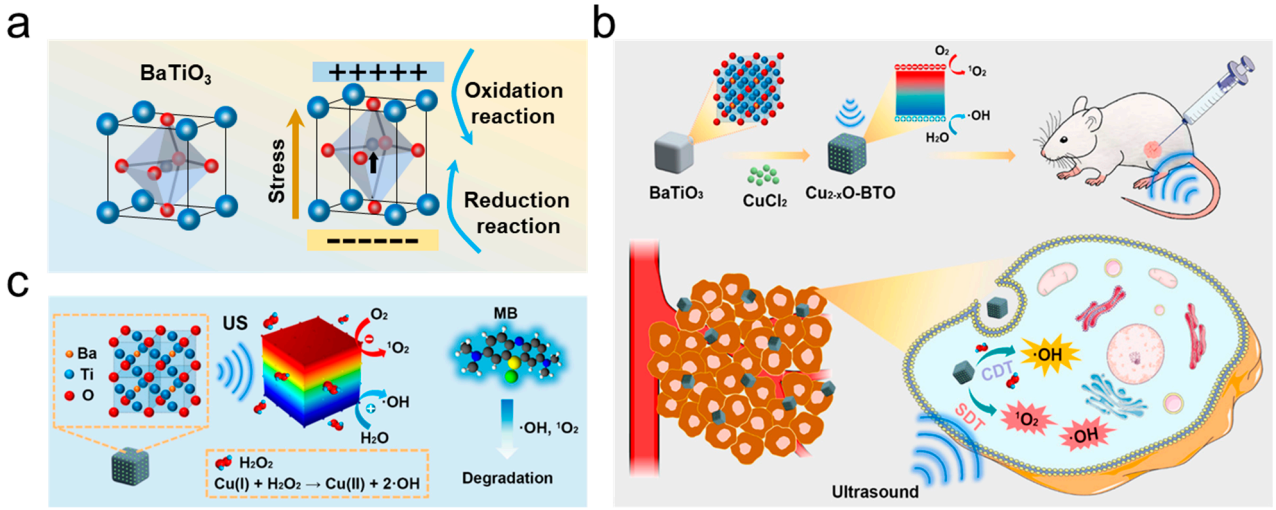


Figure 5. (**a**) Perovskite structure of barium titanate and its polarization response under applied pressure. (**b**) Schematic representation of the enhanced sonodynamic and chemodynamic therapy utilizing $Cu_{2-x}O$–BTO NCs. (**c**) Illustration depicting the impact of $Cu_{2-x}O$–BTO NCs on the degradation of methylene blue. Reproduced with permission from Ref. [60], Copyright 2022, American Chemical Society.

Wang et al. introduced a US-responsive nanocatalyst, BTO/MoS_2@CA, constructed by BTO with few-layer MoS_2 nanosheets and modifying the surface with pH-responsive cinnamaldehyde (CA) (Figure 6a) [61]. This multifunctional nanocatalyst addressed the acidic tumor microenvironment by self-supplying H_2O_2 and enhancing peroxidase (POD)-like activity under US stimulation. It was shown that the MoS_2 surface modulated electron distribution to optimize H_2O_2 decomposition (Figure 6b). The BTO/MoS_2@CA system efficiently catalyzed H_2O_2 to generate highly toxic hydroxyl radicals, depleted intracellular glutathione (GSH), and disrupted the redox balance of tumor cells. This led to lipid peroxidation, cysteine/glutamate antiporter inactivation, and ferroptosis (Figure 6c). This process achieved excellent antitumor efficacy against colon cancer in vivo with minimal side effects, with the tumor volume decreasing efficiently (Figure 6d).

Another effective approach involves the doping of BT-based materials with specific atoms, thereby introducing vacancies into their crystal lattice. This modification not only reduces the material's band gap but also significantly enhances its piezoelectric properties [62]. Deng et al. reported that palladium (Pd) doping not only lowered the hydrogenation temperature but also narrowed the band gap, thereby facilitating the separation of electron-hole pairs. Moreover, Pd exhibited dual mimetic enzymatic activity, functioning both as a peroxidase and as a catalase. This dual catalytic activity amplified ROS generation, mitigated the hypoxic TME, and ultimately enhanced therapeutic efficacy [63]. In the 4T1 tumor-bearing BALB/c mouse model, the Pd-BTO@P + US group exhibited a notable tumor growth inhibition (TGI) rate of 90.67%. Histological analysis of the major organs through H&E staining indicated no significant tissue damage, providing additional evidence of the safety of the treatment. Similarly, Zhao et al. developed a dual-function cancer therapy platform (BST@LA) combining SDT and gas therapy, utilizing L-arginine-functionalized strontium (Sr)-doped barium titanate (BST) nanoparticles. The introduction of Sr doping at the A-site of the ABO_3 perovskite structure generates oxygen vacancies, which in turn augment the intrinsic piezoelectric properties of BST. Furthermore, the reduction of the band gap enhances carrier mobility, thereby facilitating efficient ROS generation under ultrasound stimulation. In vivo experiments demonstrate the effectiveness of this strategy, showing an impressive tumor suppression rate of 89.5% in the 4T1 tumor mouse model [16].

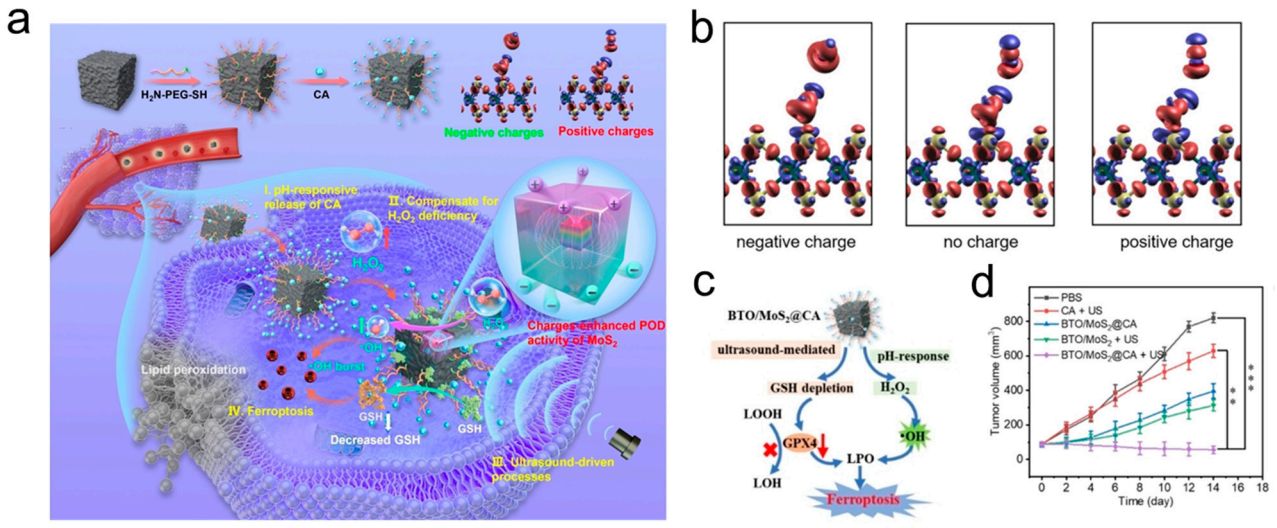


Figure 6. (**a**) Schematic diagram showing the enhancement of BTO/MoS_2@CA POD-like catalytic activity through positive and negative charge modification for efficient antitumor therapy. (**b**) Charge density distribution during the fourth step of the reaction sequence. (**c**) Schematic illustration of pH-responsive CA release and its role in ferroptosis induction. (**d**) Tumor growth inhibition curves for mice with different treatments. Significant differences between groups were indicated as *** $p < 0.001$ and ** $p < 0.01$. Reproduced with permission from Ref. [61] Copyright 2023, Wiley-VCH GmBH.

4.2. ZnO

ZnO has emerged as a prominent piezoelectric material for SDT, owing to its excellent biocompatibility, biodegradability, and capacity to generate ROS when exposed to US [54,64]. ZnO's wurtzite crystal structure, which belongs to the 6 mm point group, imparts piezoelectric and polar characteristics along the <0001> axis, often referred to as the c-axis [64]. The polarity of the material is determined by the alignment of the cation–anion bond, which runs parallel to the c-axis. Specifically, when the bond direction moves from a zinc atom to an oxygen atom (or vice versa), the [0001] direction is considered zinc- (or oxygen-) polar. The hexagonal wurtzite structure of ZnO supports the induction of polarization under mechanical stress, making it an effective sonosensitizer for cancer treatment. Furthermore, ZnO's piezoelectric and therapeutic properties have been further optimized through strategies such as doping and the formation of heterostructures.

The morphology of ZnO plays a crucial role in determining its piezoelectric and sonodynamic performance, as it directly influences the material's surface area, charge separation efficiency, and interaction with US. Morphological optimization can significantly enhance ROS generation and the overall therapeutic efficacy of ZnO-based sonosensitizers. Han et al. reported that the nanocomposites of gold nanoparticles, zinc oxide nanorods (ZnO NRs) and hydrophilic polyethylene glycol (PEG) can enhance ROS generation and effectively inhibit tumor growth of lung cancer (Figure 7a) [65]. Cai et al. reported that hollow ZnO (HZnO) nanospheres, when combined with black phosphorus quantum dots and PEG, not only enhanced the piezoelectric effect but also improved tumor-targeting ability [17]. ZIF-8 with a diameter of 40 nm was synthesized and used as a precursor to prepare ZnO nanospheres by pyrolysis and self-assembly in a methanol/ethanol (1:1) solution (Figure 7b). By introducing different amounts of water into the above system, the solid ZnO nanospheres gradually changed to hollow structures (Figure 7c). The hollow structure of HZnO facilitated deformation under US mechanical force, increasing ROS generation. This approach also ensured that ZnO degraded in an acidic tumor microenvironment, releasing Zn^{2+} and PO_4^{3-} ions to induce pro-death autophagy, adding another layer of

therapeutic efficacy (Figure 7d). In a 4T1 tumor-bearing mouse model, the tumor inhibition rate of the HZnO-BPQDs/US group was inhibited significantly (90%). In addition, a flying-saucer-shaped nanoheterojunction has been designed by coating copper oxide (Cu_xO) onto the surface of PEGylated ZnO nanoparticles [18]. Under US exposure, the resulting Cu_xO@ZnO nanoheterojunctions demonstrated enhanced motility, which aided in the penetration of colorectal mucus, deep tumor invasion, and internalization by tumor cells. The incorporation of Cu_xO prevented the rapid recombination of electrons and holes, thereby facilitating the generation of ROS. Following rectal administration, the combination of Cu_xO@ZnO and PD-L1 antibodies significantly inhibited the growth of both orthotopic and distant tumors of colorectal cancer.

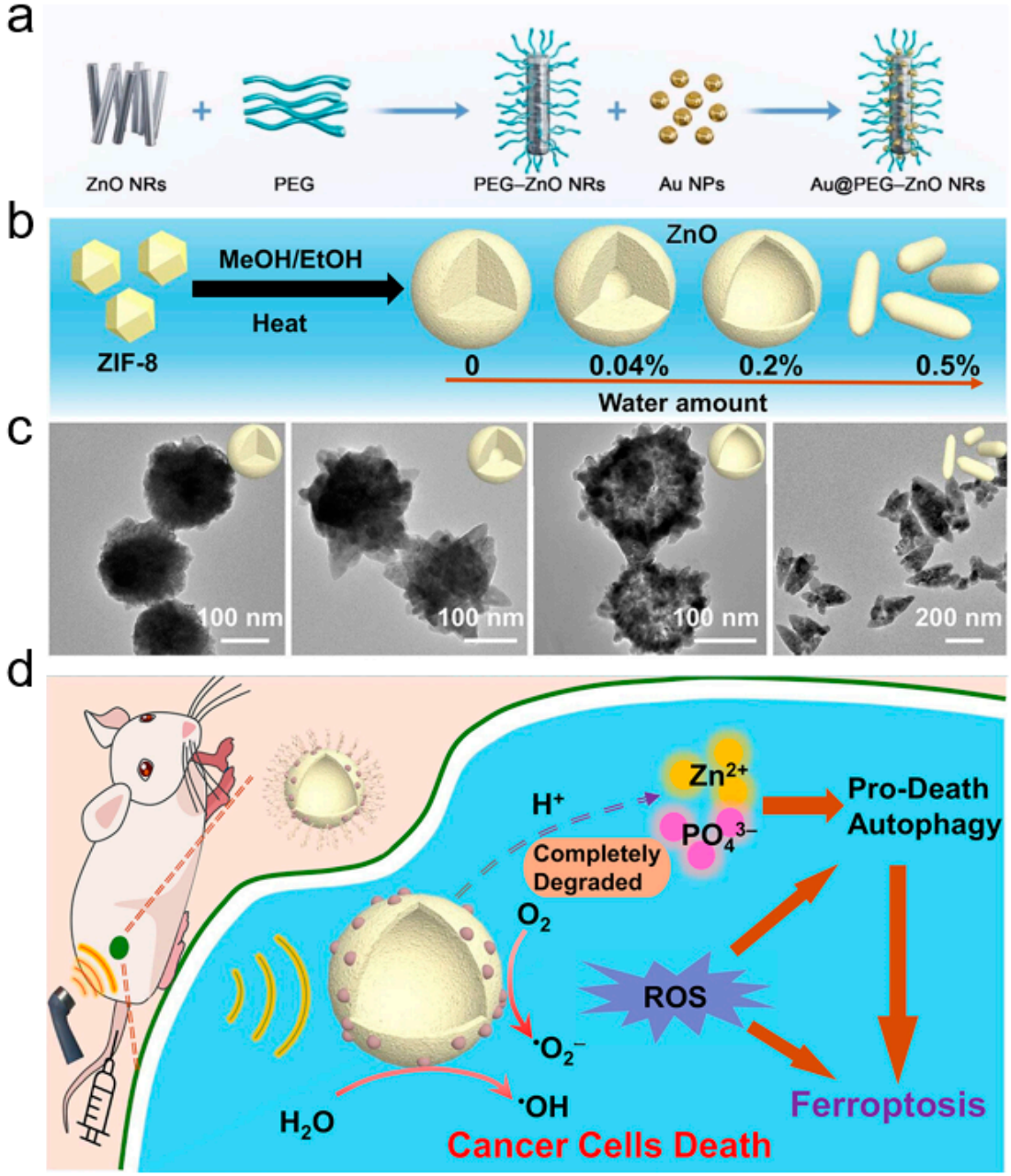


Figure 7. (**a**) Design of Au@PEG-ZnO nanocomposites. Reproduced with permission from Ref. [65], Copyright 2024, Elsevier. (**b**) Schematic of HZnO preparation. (**c**) TEM images of ZnO with different contents of water in the reaction process. (**d**) Schematic of HZnO-BPQDs-PEG in anti-tumor process through Zn^{2+}/PO_4^{3-} ions-induced pro-death autophagy and ROS. Reproduced with permission from Ref. [17], Copyright 2024, Elsevier.

Oxygen vacancies in ZnO play a crucial role in enhancing its sonodynamic performance by promoting charge separation and increasing the production of ROS. For instance, ZnO/kaolinite composites rich in oxygen vacancies exhibited spontaneous ROS generation even in the absence of external light stimuli, making them particularly effective in hypoxic tumor environments. This intrinsic ROS production capability not only amplified the cytotoxic effects on tumor cells but also ensured high biocompatibility [66]. Tian et al. developed biodegradable, porous Mn-doped ZnO (Mn-ZnO) nanoclusters with an enhanced piezoelectric effect through doping engineering [67]. The Mn-doping process induced lattice distortion, which increased polarization, and simultaneously created abundant oxygen vacancies that prevented the recombination of electron-hole pairs. This resulted in efficient ROS generation when subjected to ultrasound irradiation.

While ZnO is generally recognized as safe by the U.S. Food and Drug Administration (FDA) for inclusion in sunscreens and topical skin ointments, its nanoscale formulation raises concerns about potential toxicity, particularly neurotoxicity [68]. Studies have shown that ZnO NPs can cross the blood-brain barrier (BBB) and accumulate in neural tissues, potentially leading to oxidative stress, mitochondrial dysfunction, and neuroinflammation [69,70]. The dissolution of ZnO NPs into Zn^{2+} ions plays a crucial role in their cytotoxic effects, as excessive intracellular Zn^{2+} can disrupt neuronal homeostasis, induce apoptosis, and contribute to neurodegenerative processes. Moreover, high concentrations of ZnO NPs have been associated with inflammatory responses in brain microglial cells, which could exacerbate neuronal damage. To mitigate these risks, strategies such as surface modifications, controlled degradation, and optimized dosing regimens are essential for ensuring the safe biomedical application of ZnO-based piezoelectric sonosensitizers. Future studies should focus on evaluating long-term neurotoxicity and biodistribution to facilitate clinical translation.

4.3. $BiFeO_3$

Multiferroic materials, characterized by the simultaneous presence of two or more ferroic orders, have garnered significant attention in materials science due to their potential in facilitating the development of innovative multifunctional devices [71]. Among these materials, Bismuth Ferrite ($BiFeO_3$, BFO) stands out as particularly noteworthy due to its unique fusion of ferroelectric and antiferromagnetic properties, both of which coexist at room temperature. The ability of BFO to support both electric and magnetic orderings concurrently, coupled with their remarkable optical, piezoelectric, and magnetoelectric coupling capabilities, positions it as a highly promising candidate for a diverse range of technological applications [72]. BFO exhibits a perovskite crystal structure, with a substantial remnant polarization and high Curie (~1100 K) and Néel (~640 K) temperatures, making it stable across a broad temperature range.

The intrinsic properties of BFO, such as high polarization, stable piezoelectric response, and a suitable bandgap for ROS generation, render it an appealing candidate for SDT. For instance, the development of a BFO-BT solid solution optimized its piezoelectric properties and band structure, achieving enhanced ROS production and alleviating tumor hypoxia through a piezo-Fenton process while integrating SDT and CDT for synergistic effects for treating melanoma [20]. Similarly, the incorporation of BFO nanosheets into a ROS-sensitive hydrogel scaffold demonstrated significant potential for piezocatalytic immunotherapy by inducing ICD and reversing the immunosuppressive tumor microenvironment, thus promoting long-term immune memory against breast cancer [19]. Moreover, Ce doping in BFO nanoparticles further amplified piezoelectric performance by improving charge separation and catalytic activity, enabling the combination of CDT, SDT, and piezodynamic therapy (PzDT) for breast tumor ablation [73]. These advancements collectively highlight

BFO and its derivatives as versatile and effective sonosensitizers, capable of addressing tumor hypoxia and achieving multimodal therapeutic outcomes in cancer treatment.

4.4. MoS_2

MoS_2, a classic two-dimensional transition metal dichalcogenide, is known for its distinctive layered structure [74]. The piezoelectric behavior of MoS_2 is intricately linked to its crystallographic structure, with d_{33} values ranging from 1 to 4 pm V^{-1}. The piezoelectric characteristics of MoS_2 stem from the polarization of M-S dipoles, wherein the Mo and S atoms are symmetrically positioned at the vertices of the honeycomb structure. Each unit cell comprises a singular Mo atom and two S atoms (2S-Mo) [75]. This inherent spatial asymmetry gives rise to spontaneous polarization in the strain-free state. Upon tensile deformation, the 2S-Mo dipole is stretched, inducing polarization that orients from sulfur to molybdenum. In contrast, when subjected to compressive forces, the direction of the induced polarization is reversed. This polarization phenomenon endows MoS_2 with significant in-plane piezoelectricity [56]. Consequently, the inherent structural characteristics of MoS_2 endow it with distinct advantages for piezoelectric applications. In addition to its ease of exfoliation and high specific surface area, the layered structure of MoS_2 plays a crucial role in its piezoelectric behavior. This distinct configuration enables MoS_2 to efficiently generate internal electric fields when subjected to mechanical stress, facilitating the separation of electron-hole pairs and enhancing the production of ROS for SDT therapeutic purposes. Xia et al. demonstrated the use of multifunctional MoS_2 nanosheets, which combine intrinsic plasmonic properties with piezocatalytic activity, in image-guided synergistic tumor therapy [76].

To improve piezoelectric performance, Wu et al. incorporated sulfur vacancies into MoS_2 nanoflowers, creating Sv-MoS_2 (Figure 8a,b) [77]. Under US stimulation, Sv-MoS_2 induced piezoelectric polarization and band tilting, which facilitated the separation and migration of charge carriers, thereby enhancing catalytic reactions, promoting the production of ROS and augmenting the efficacy of SDT. In the 4T1 tumor-bearing mice, the Sv-MoS_2 NF + US groups showed considerable tumor suppression, with tumor inhibition rates of 85.4% (Figure 8c), while maintaining favorable biocompatibility. However, the piezoelectric performance of MoS_2 faces significant challenges related to its stability, which can be compromised by environmental conditions and prolonged usage. Although MoS_2-based materials generally exhibit commendable biocompatibility, precise quantification of their piezoelectric properties remains a complex task, and the fabrication of high-quality MoS_2 piezoelectric materials remains technically demanding. Future research should prioritize enhancing stability, developing accurate quantification techniques, and optimizing fabrication methods for MoS_2-based materials, thereby advancing their applicability and facilitating their further development in therapeutic applications.

4.5. Bi-Based Nanomaterials

Bismuth (Bi), positioned as the 83rd element on the periodic table, is a pnictogen semimetal with a notably high atomic number (Z), often associated with toxic heavy metals. However, Bi and its derivatives are regarded as relatively less toxic, earning them the classification of a "green element" due to their reduced environmental and biological risks [78]. In the realm of cancer therapy, Bi-based nanoparticles have undergone significant evolution, progressing from binary nanoparticles and organometallic-encapsulated polymeric constructs to ternary nanoparticle formulations and Bi-based complexes. This progression culminated in the development of elemental Bi nanoparticles, which have demonstrated substantial promise in SDT. Their intrinsic piezoelectric properties enable the generation of polarization charges upon ultrasound exposure, facilitating efficient charge separation

and enhancing electron-hole pair formation. This, in turn, significantly amplifies ROS production, thereby optimizing the therapeutic efficacy of SDT [79–81].

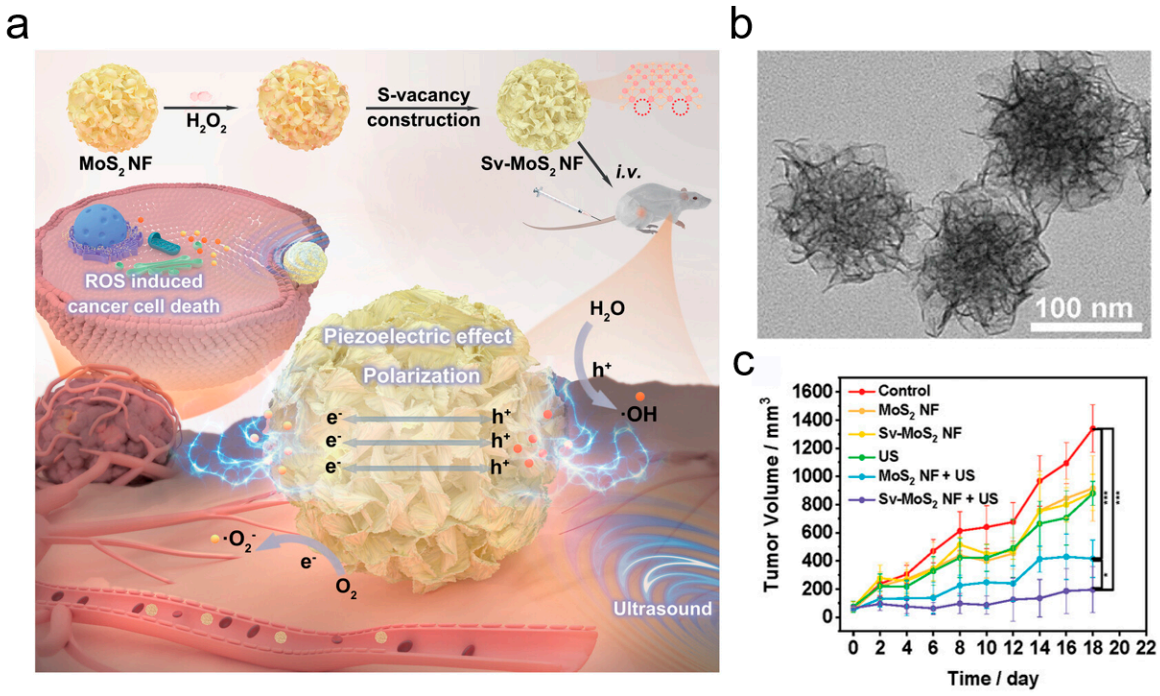


Figure 8. (**a**) Schematic of vacancy-induced piezoelectric SDT. (**b**) TEM image of MoS_2 NF. (**c**) Tumor volume progression across different treatment groups over an 18-day therapeutic period. Significant differences between groups were indicated as *** $p < 0.001$ and * $p < 0.05$. Reproduced with permission from Ref. [77], Copyright 2023, Wiley-VCH GmBH.

2D Bi-based materials, such as Bi_2WO_6, Bi_4NbO_8Br, BiOCl, and Bi_2MoO_6, have emerged as promising candidates for SDT owing to their layered structures, which facilitate efficient charge separation and the generation of ROS [82–87]. For instance, a bimetallic Bi_4NbO_8Br polyvinylpyrrolidone (BNOBP) composite with a narrow bandgap (2.45 eV) has been synthesized as a piezoelectric sonosensitizer (Figure 9a) [84]. The interactions between the Bi–O and Nb–O layers helped narrow the bandgap, which promoted carrier transfer and accelerated electron-hole separation. Compared to other materials like TiO_2 and BiOBr, BNOBP exhibited a faster acoustoelectric response. Additionally, BNOBP can mitigate the overexpression of GSH in tumors, preventing ROS scavenging by GSH. Therefore, in 4T1 tumor-bearing mice, BNOBP effectively inhibited the growth of tumors under US irradiation (inhibition rate of ~80%). Additionally, no significant damage occurred to the heart, liver, spleen, lungs, and kidneys. Similarly, ultrathin Fe-doped bismuth oxychloride nanosheets (BOC-Fe NSs) have been developed as piezoelectric sonosensitizers for SDT (Figure 9b) [85]. The oxygen vacancies present in BOC-Fe NSs functioned as electron trapping sites, further promoting the separation of electrons and holes, thereby boosting ROS production under ultrasound exposure. In addition to their piezoelectric properties, BOC-Fe NSs also facilitated ROS generation through a Fenton reaction catalyzed by Fe ions, utilizing endogenous H_2O_2 in tumor tissues to contribute to CDT. In vivo SDT against 4T1 breast cancer showed that the inhibition rate of the BOC-$Fe_{0.1}$ NSs + US group was as high as 90%. Furthermore, Dong et al. designed the thin-layer 2D Bi_2MoO_6-PEG nanoribbons (BMO) that effectively depleted endogenous GSH in cancer cells, disrupting redox homeostasis and thereby enhancing ROS production efficiency against cervical cancer (Figure 9c) [86]. In the U14 tumor model, mice receiving BMO NRs combined with ultrasound irradiation exhibited significant tumor suppression, reaching an

inhibition rate of 96.6%. To assess the long-term in vivo safety of BMO NRs, hematological, blood biochemical, and histopathological evaluations were conducted, revealing minimal adverse effects and excellent biocompatibility.

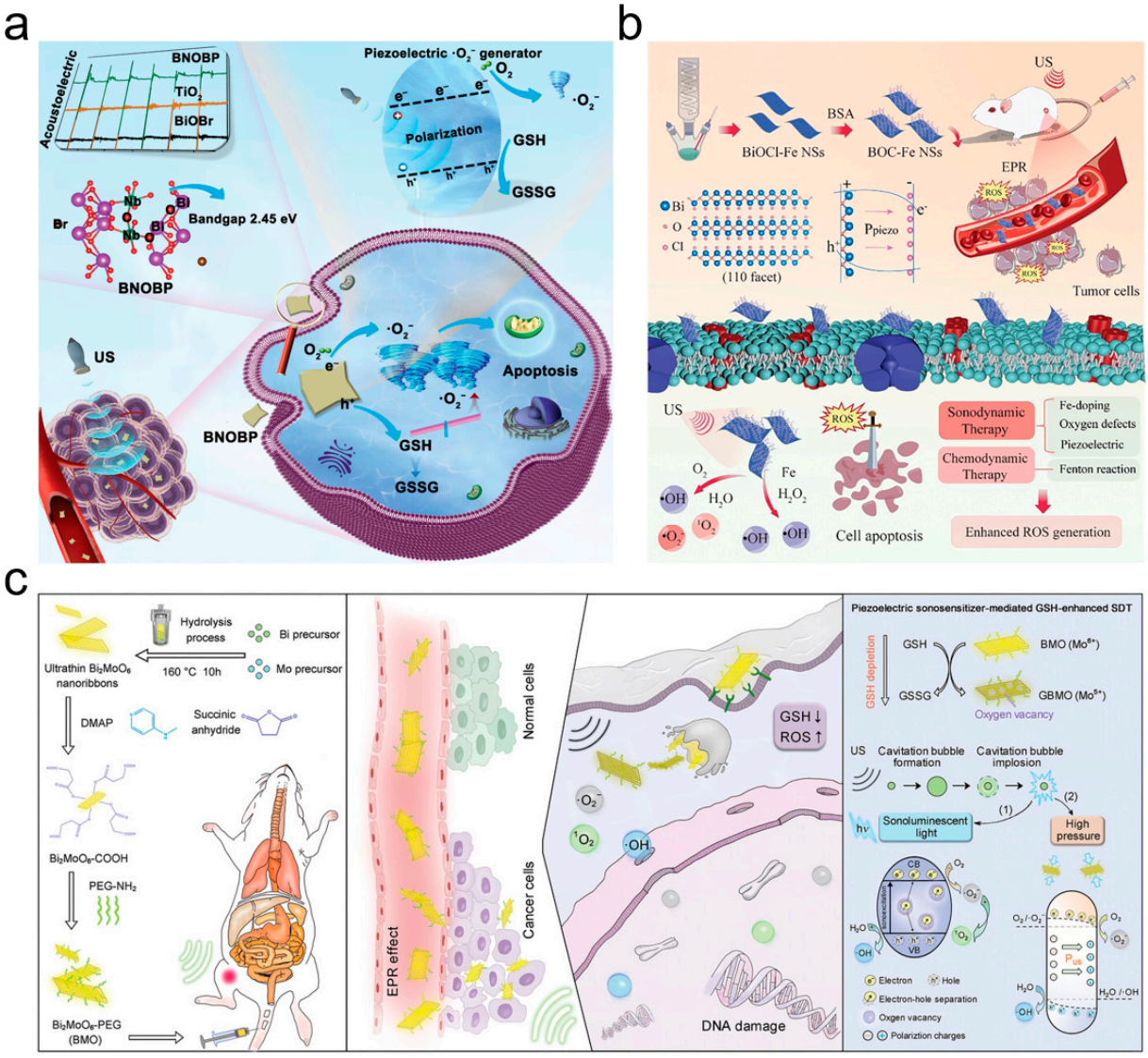


Figure 9. (**a**) Schematic representation of a US-driven bimetallic small bandgap piezoelectric·O_2^- generator designed to enhance SDT. Reproduced with permission from Ref. [84], Copyright 2024, Wiley-VCH GmBH. (**b**) Schematic illustration the development of iron-doped BiOCl NSs coated with BSA as the sonosensitizer for enhanced tumor SDT. Reproduced with permission from Ref. [85], Copyright 2023, Wiley-VCH GmBH. (**c**) Schematic diagram of the 2D piezoelectric Bi_2MoO_6 sonosensitizer for GSH-enhanced SDT. Reproduced with permission from Ref. [86], Copyright 2021, Wiley-VCH GmBH.

Bi-based nanomaterials possess a diverse array of properties, including exceptional piezoelectric performance, remarkable stability, large surface areas, pronounced paramagnetism, excellent catalytic activity, ease of functionalization, low toxicity, and cost-effectiveness. These attributes render them particularly well-suited for SDT in oncological applications. Although research on Bi-based piezoelectric nanomaterials remains in the nascent stages, their outstanding properties signal significant potential within the biomedical domain, especially in the context of cancer treatment. The synergy between their piezoelectric characteristics and high biocompatibility establishes Bi-based piezoelectric

materials as a promising therapeutic modality, opening new avenues for future cancer therapies and research.

5. Piezoelectric SDT-Based Nanomedicines for Cancer Immunotherapy

Cancer is a highly intricate and dynamic ecosystem composed not only of tumor cells, but also diverse non-cancerous cells embedded within a complex, vascularized extracellular matrix (ECM). The TME plays a pivotal role in tumor progression, influencing key processes such as angiogenesis, invasion, metastasis, and drug resistance. The TME is not a passive backdrop. It interacts actively with cancer cells through various signaling pathways, creating a reciprocal relationship that fosters cancer progression and therapy resistance [88]. This crosstalk between cancer cells and the surrounding non-cancerous cells within the TME often leads to the creation of an immunosuppressive microenvironment, further complicating effective treatment strategies. SDT can assist in boosting antitumor immunotherapy by modulating the TME, reshaping immune cell function, and reprogramming the immune landscape [7]. Significantly, SDT has emerged as a powerful modality for inducing ICD, a process that stimulates a systemic anti-tumor immune response. This approach, referred to as sono-immunotherapy, harnesses the ability of sonosensitizers to enhance SDT's therapeutic efficacy while inducing a potent immune response. For instance, while effector $CD8^+$ T cells are recruited to the TME during SDT, their cytotoxic functions are often impaired in tumors characterized by an "immune-cold" environment. These tumors contain a variety of immunosuppressive cells, such as regulatory T (Treg) cells and M2-polarized tumor-associated macrophages (TAMs), which inhibit the activity of $CD8^+$ T cells. In such environments, T cells may survive but become exhausted, a state referred to as exhausted T cells (Tex cells), leading to diminished anti-tumor activity [89]. To overcome these challenges, SDT is increasingly being combined with other therapeutic modalities, such as immune checkpoint inhibitors or targeted therapies, to improve T cell functionality and promote an anti-tumor immune response. Additionally, the use of nan-osonosensitizers that can reprogram the TME, deplete immunosuppressive cells, and induce ICD is paving the way for more effective sonodynamic immunotherapies with improved outcomes in cancer treatment.

5.1. Mechanism of Cancer Immunotherapy

The immune response can be categorized into two primary mechanisms: humoral immunity and cell-mediated immunity. In the realm of anti-tumor immunotherapy, cell-mediated immunity, particularly T cell-mediated responses, assumes a pivotal role. This immune cascade unfolds through a series of orchestrated events, collectively known as the "cancer-immunity cycle", a self-perpetuating and iterative process that is indispensable for the initiation and amplification of the immune system's capacity to target and eliminate cancer cells [90,91]. Within this cycle, tumor cells undergoing apoptosis or necrosis release tumor-associated antigens (TAAs) and co-stimulatory signals. These antigens are captured by antigen-presenting cells (APCs), which then process them into smaller peptide fragments. These peptides are subsequently presented in major histocompatibility complex class I (MHC-I) or class II (MHC-II) molecules, forming peptide-MHC complexes. The APCs are then activated through co-stimulatory signaling, maturing into fully functional antigen-presenting cells. These mature APCs migrate to the draining lymph nodes, where they engage naïve T cells, presenting the peptide-MHC complexes and triggering T cell activation. This interaction initiates the differentiation of CTLs, which undergo clonal expansion, enter the bloodstream, and home to the tumor site. There, the CTLs recognize and eliminate malignant cells through the release of cytotoxic molecules, such as granzyme B and perforin. The subsequent destruction of tumor cells releases additional TAAs and

co-stimulatory signals, further propagating and intensifying the immune response, thereby reinforcing the adaptive immune system's capacity to fight cancer.

Cancer sono-immunotherapy can be broadly classified into two distinct approaches: ICD-based sono-immunotherapy and combinatorial sono-immunotherapy, each targeting specific immunological signaling pathways to bolster the anti-tumor immune response [7,92,93]. ICD-based sono-immunotherapy leverages the capacity of SDT to induce ICD, a process in which tumor cells release DAMPs. These DAMPs play a crucial role in activating the immune system, triggering the release of TAAs, and thereby initiating both local and systemic immune responses. By inducing direct cytotoxicity and simultaneously fostering antigen presentation, ICD-based therapies promote the activation of various immune cells, enhancing the body's capacity to target and eliminate malignant cells. In contrast, combinatorial sono-immunotherapy combines SDT with a range of immunomodulatory agents designed to further amplify the immune response. These agents include inhibitors of the PD-1/PD-L1 checkpoint pathway, TLR agonists, stimulator of interferon genes (STING) agonists, indoleamine-2,3-dioxygenase (IDO) inhibitors, and various immunomodulatory cytokines. The synergistic effects of SDT and these therapeutic agents work to not only activate effector immune cells, such as CTLs, but also inhibit immunosuppressive cells, including Tregs and M2-polarized TAMs. This dual approach enhances the overall immune response, rendering the tumor microenvironment more conducive to immune-mediated eradication of cancer.

5.2. SDT Induced Immunogenic Cell Death

Recent investigations have elucidated that such forms of cell death can indeed induce ICD, a process marked by the translocation of CRT to the surface of dying tumor cells. CRT functions as an "eat me" signal, promoting the secretion of pro-inflammatory cytokines that facilitate the recruitment of APCs. Concurrently, dying tumor cells release DAMPs, which serve as "find me" signals, initiating a cascade of anti-tumor immune responses. ICD has thus emerged as a promising immunotherapeutic strategy for cancer treatment. The clinical application of ICD in chemotherapy and radiotherapy remains hindered by significant limitations, particularly the systemic toxicity associated with these treatments, which are often poorly tolerated by patients. SDT have demonstrated a more favorable immune profile, as the sensitizers in these therapies selectively induce cytotoxicity only upon exposure to US. Notably, SDT possesses the unique ability to enhance immunogenicity via a caspase-independent programmed necrosis pathway, further amplifying its therapeutic potential in cancer immunotherapy. Consequently, SDT holds considerable promise as a dual-purpose approach for direct tumor cytotoxicity and subsequent immune activation, a concept now recognized as sonodynamic immunotherapy.

Li et al. utilized tin monosulfide nanoparticles (SnS NPs) as nano-sonosensitizers to overcome the stromal barriers associated with desmoplastic triple-negative breast cancer (TNBC). In mouse models of TNBC and hepatocellular carcinoma (HCC), combining SDT with enhanced cytotoxic T lymphocyte infiltration resulted in significant anti-tumor effects [94]. The SSN-mediated piezoelectrocatalytic generation of H_2 helped to overcome tumor-induced immunosuppression by down-regulating the overexpression of PD-L1 on tumor cells. Concurrently, LA depletion activated $CD8^+$ T cells by inhibiting regulatory T cells, thereby co-activating tumor immunity. In an in vivo orthotopic hepatoma model with deep-seated tumors, SSN combined with ultrasound significantly suppressed tumor progression. Throughout the 28-day treatment period, all treated mice exhibited a 100% survival rate. In another study, Qian et al. introduced an oxygen-deficient piezoelectric-photothermal sensitizer, bismuth vanadate nanorods (BVP) supported by platinum nanodots [95]. The coordination of bismuth ions with glutathione further amplified oxidative stress within tumor cells. The heat and ROS generated through this approach denatured collagen in

the ECM, improving the penetration of BVP into 4T1 breast tumors while simultaneously inducing ICD. This "degeneration and penetration" strategy, combined with photoacoustic therapy, effectively activated immune cells and inhibited both tumor growth and metastasis. In vivo experiments of 4T1 tumor-bearing mice showed that the activation rates of $CD8^+$ T cells in the spleen and lymph nodes of the synergy group were 31.3% and 35.4%, respectively, demonstrating a significant enhancement of immune response.

5.3. Combinational Sonoimmunotherapy

SDT and immune checkpoint inhibition (ICI) represent two pioneering strategies in cancer treatment, and when combined, they offer a powerful synergistic approach for combating tumors. ICIs, including anti-PD-1 and anti-PD-L1 antibodies, block the inhibitory signals that cancer cells use to escape immune detection. By reactivating exhausted T cells, ICIs restore the immune system's ability to recognize and eliminate cancer cells. Nevertheless, ICIs alone may not be sufficient for tumors with low immunogenicity or insufficient T-cell infiltration. This limitation has driven the exploration of combining ICIs with therapies like SDT to boost their therapeutic effectiveness.

Preclinical studies have shown the potential of this combination therapy in achieving durable anti-tumor immunity. For instance, US-triggered ROS production by sonosensitizers has been found to increase T-cell infiltration while concurrently decreasing the expression of immune checkpoint molecules such as PD-L1. This dual modulation of the immune landscape not only promotes tumor regression but also reduces the likelihood of metastasis and recurrence. For example, ultrathin $CaBi_2Nb_2O_9$ nanosheets with tunable oxygen vacancies (CBNO-OV1) were prepared for synergistic necroptosis and immunotherapy (Figure 10a) [62]. CBNO-OV1 induced necroptosis through the explosive release of ROS, which, in turn, triggered a robust immune response in vivo. Specifically, necroptosis activated macrophage M1 polarization via the NF-κB signaling pathway, thereby promoting T-cell differentiation. Treatment with either CBNO + US or CBNO-OV1 + US resulted in a significant upregulation of M1 markers, with elevated expression of CD86 (Figure 8b). Notably, the proportion of $CD86^+$ macrophages in the CBNO-OV1 + US group was more than threefold higher than that in the control group (Figure 10b). Immunofluorescence staining corroborated these findings (Figure 10c), further confirming that the CBNO-OV1 + US combination markedly enhanced T-cell activation. In a bilateral tumor model in mice, the V/V_0 values for tumor volume were 14.3 in the Control group, 3.7 in the CBNO + US group, and 1.1 in the CBNO-OV1 + US group. Additionally, the treatment effectively suppressed both primary and distant tumor growth.

Pu et al. introduced an innovative 2-deoxyglucose (2-DG) and bismuth ferrite co-loaded gel (DBG) scaffold aimed at enhancing piezocatalytic immunotherapy for cancer (Figure 10d) [19]. Upon exposure to US irradiation, DBG generated both ROS and piezoelectric signals, effectively triggering anti-tumor immune responses. Moreover, the ROS-sensitive release of 2-DG disrupted N-glycan synthesis, thereby mitigating the immunosuppressive tumor microenvironment. Phagocytic activity was quantitatively assessed by analyzing the proportion of CFSE/PE double-positive cells. The DBG + US treatment resulted in a significant increase in the phagocytosis index, more than doubling the value compared to the BG + US treatment. This enhancement is attributed to the inhibition of N-glycosylation induced by 2-DG release, which facilitated the uptake of RAW 264.7 cells (Figure 10e). Additionally, increased immune cell infiltration into the tumor site in the DBG + US group provided further evidence of an activated anti-tumor immune response (Figure 10f). The synergistic effects of ultrasound stimulation and glycosylation inhibition were validated across four distinct mouse cancer models. This combination therapy established a "hot" tumor-immune microenvironment, effectively suppressing tumor growth

and lung metastases while inducing a robust immune memory response, thereby offering long-term protection against tumor recurrence.

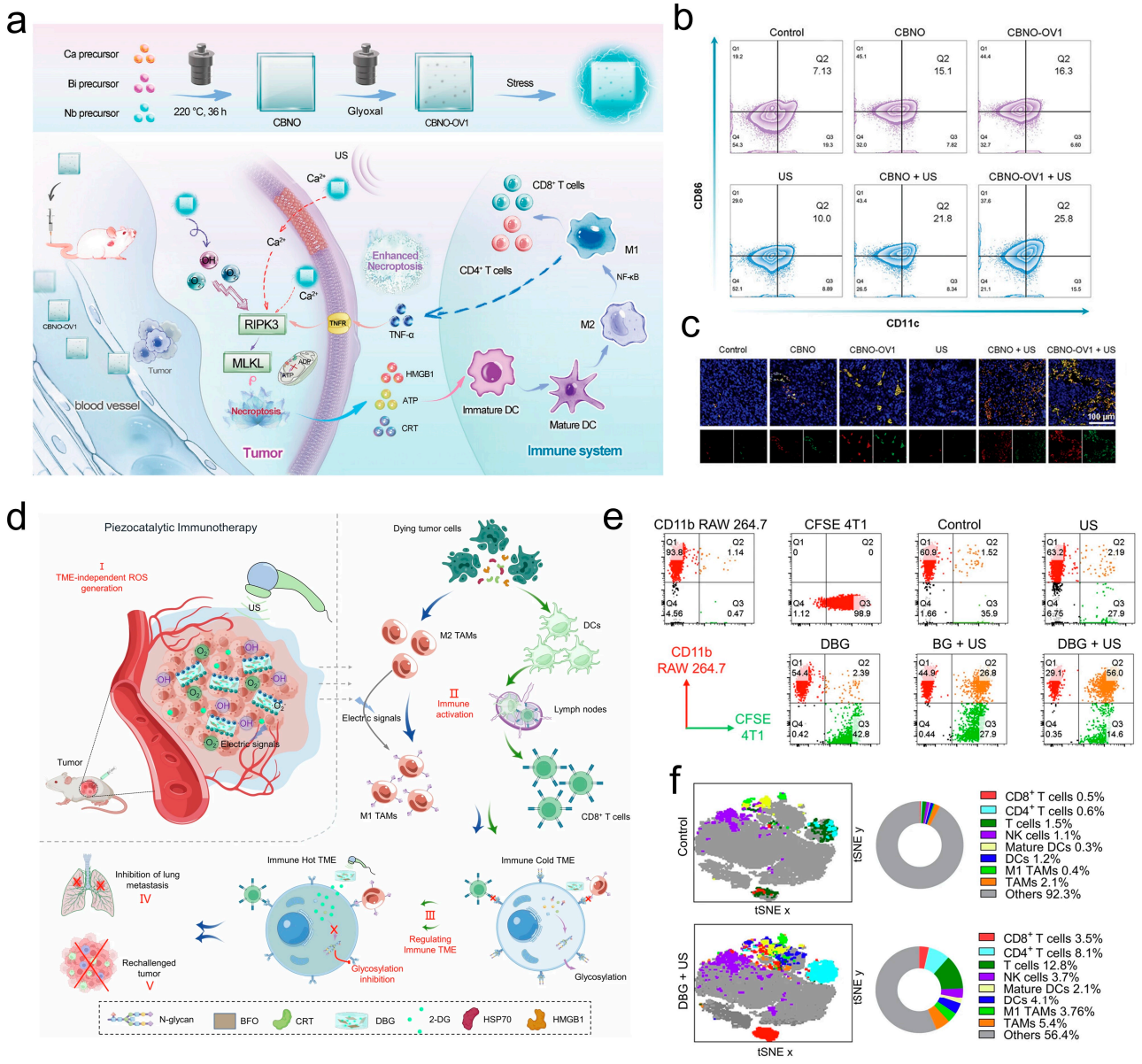


Figure 10. (**a**) Schematic representation of the synthesis of CBNO-OV1 NSs and their anti-tumor mechanism, which induces necroptosis in tumor cells, activates an immune response, and further amplifies necroptosis through immunotherapy. (**b**) Flow cytometry analysis for the detection of mature DCs marked by $CD11c^+$, $CD80^+$, and $CD86^+$ expression. (**c**) Immunofluorescence images showing nuclear staining (blue), anti-CD3 antibody staining (green), and anti-CD8 antibody staining (red) in primary tumor sections. The increased red fluorescence intensity indicates immune system activation. Reproduced with permission from Ref. [62], Copyright 2023, Wiley-VCH GmBH. (**d**) Schematic of amplified tumor piezocatalytic immunotherapy by DBG, achieved through in situ ROS generation and the inhibition of tumor cell glycosylation. (**e**) Phagocytosis ratio of 4T1 cancer cells quantified by flow cytometry. (**f**) tSNE visualization and quantification of immune cell populations in rechallenged tumors from 4T1 tumor-bearing BALB/c mice following different treatments. Reproduced with permission from Ref. [19], Copyright 2024, Springer Nature.

6. Synergistic Effects of Piezoelectric SDT-Based Nanomedicines and Other Therapies

To further improve the effectiveness of SDT, researchers have investigated the combined impact of piezoelectric SDT with various therapeutic strategies, including PDT, chemodynamic therapy (CDT), chemotherapy, and radiotherapy. The distinctive physical characteristics of piezoelectric materials allow them to integrate seamlessly with other treatments, resulting in notable synergistic effects that enhance therapeutic efficacy and support patient recovery. In combined SDT-based treatments, some materials may not initially exhibit strong piezoelectric properties during early-stage evaluations. However, this does not preclude their future potential in SDT-enhanced therapy. Ongoing interdisciplinary research and advancements in materials science continue to explore the latent piezoelectric properties of these materials, aiming to expand their applications and optimize SDT effectiveness.

6.1. Combined with Photodynamic Therapy

PDT is an FDA-approved anticancer therapy that relies on photophysical and photochemical mechanisms to activate photosensitizers, generating cytotoxic ROS [96]. It has been clinically applied to treat various malignancies, including lung, esophageal, bladder, and skin cancers, as well as precancerous conditions such as actinic keratosis and Barrett's esophagus. Piezoelectric semiconductors (PS) are a unique class of materials that possess both semiconductor and piezoelectric properties, enabling them to respond sensitively to external stimuli such as light, electricity, and mechanical force [97,98]. This responsiveness allows for effective modulation of charge carrier separation, transport, and recombination. When photoexcited piezoelectric materials interact with a solution, photoinduced carriers migrate through the solid–liquid interface, leading to an upward bending of the energy band [99]. This band bending acts as a barrier to electron transfer in reduction reactions while facilitating hole transfer in oxidation reactions. Upon exposure to ultrasound vibrations, the piezoelectric effect generates polarized charges that spontaneously form an internal electric field. This field alters the energy band structure: the surface with positive polarization experiences downward band bending, promoting electron migration into the electrolyte (reducing the reductive potential) and suppressing hole migration (increasing the oxidative potential). Conversely, the surface with negative polarization exhibits upward band bending, further inhibiting electron transfer while enhancing hole migration. This synergistic process, known as piezo-photocatalysis, enhances charge carrier dynamics and expands the potential applications of PS in catalytic and biomedical fields.

Piezo-photocatalysis has recently emerged as a promising strategy for converting light and mechanical energy, classified into two main types: (1) integrated piezo-photocatalysts, where a single material exhibits both piezoelectric and photosensitive properties, and (2) hybrid piezo-photocatalysts, consisting of two distinct components. For instance, natural sphalerite nanosheets (NSH700 NS) serve as an integrated piezo-photocatalyst, demonstrating efficient generation of $\bullet O_2^-$ and •OH while depleting glutathione (GSH) under simultaneous ultrasound and laser irradiation. Systematic in vitro cellular studies and in vivo xenograft tumor models have confirmed the exceptional tumor elimination capability of this method, primarily attributed to a substantial ROS surge and consequent DNA damage.

However, the limited tissue penetration depth of laser light poses a challenge for treating deep-seated tumors. Cong et al. proposed an alternative approach using g-C_3N_4/Pt/Luminol@cytomembrane (CPL@M) to achieve in situ chemiluminescence activation. In response to the high H_2O_2 levels within the TME, CPL@M emitted ultraviolet-visible (UV–vis) light in the 400–550 nm range, catalyzing water splitting via g-C_3N_4/Pt

and subsequently reducing tumor interstitial fluid pressure [100]. Meanwhile, the piezoelectric nature of CPL@M enabled deformation under ultrasound stimulation, generating an internal electric field that directed photogenerated electrons and holes to opposite sites. Consequently, O_2 was converted into $\bullet O_2^-$ and $^1O_2$ by the transferred electrons. The resulting ROS further oxidized Pt into Pt^{2+}, while the reduced interstitial fluid pressure facilitated convective diffusion, ultimately enhancing Pt-based chemotherapy for effective tumor cell eradication. Zhang et al. designed orthorhombic $ZnSnO_3$ quantum dots (QDs) with piezo-photoelectronic effects encapsulated in hexagonal upconversion nanoparticles ($ZnSnO_3$@UCNPs) [101]. The 980 nm near-infrared light enables deep penetration, while the watermelon-like structure ensures efficient Förster resonance energy transfer. Under ultrasonic and NIR laser activation, heat and pressure deform UCNPs, inducing $ZnSnO_3$ QD deformation and generating isotropic micro-electric fields. This enhances the internal electric field, suppressing charge recombination and improving piezocatalytic performance. In 4T1 tumor-bearing mice, the $ZnSnO_3$@UCNPs + US + NIR group achieved the highest tumor inhibition rate (98.8%).

The combination of PDT and SDT remains relatively uncommon, as both therapies function through ROS generation, leading to overlapping mechanisms. While piezoelectric effects hold great potential in various treatments, their synergy with PDT has been less explored. Due to ultrasound's superior tissue penetration compared to light, the combined application of both does not significantly enhance therapeutic efficacy, resulting in limited synergistic benefits.

6.2. Combined with Chemodynamic Therapy

CDT leverages the weak acidity and excess H_2O_2 in the TME to trigger Fenton or Fenton-like reactions, generating •OH to disrupt key tumor cell structures, ultimately causing cell death [102]. Combining piezoelectric SDT with CDT amplifies antitumor effects through multiple synergistic pathways. Ultrasound-activated SDT produces ROS like $^1O_2$ and O_2^-, which enhance H_2O_2 generation, thereby accelerating the Fenton reaction and increasing •OH production. CDT depletes GSH, weakening tumor antioxidant defenses, while the piezoelectric effect further disrupts tumor metabolism, improving therapeutic sensitivity. This light-independent approach is effective for deep tumors and can trigger ICD to boost antitumor immunity.

Wang et al. developed metformin–DSPE-PEG20000@$BaTiO_3$ and Fe_3O_4 (Met@BF), a nanocomposite featuring pH and ultrasound dual responsiveness with charge-reversal properties [103]. In circulation, Met@BF remains negatively charged but switches to a positive charge in the tumor's acidic microenvironment, facilitating deep penetration and accumulation. Under ultrasound, $BaTiO_3$ catalyzes H_2O_2 production, fueling the Fe_3O_4-driven Fenton reaction to generate •OH, which enhances tumor destruction. Additionally, •OH induces ICD, releasing DAMPs to activate antitumor immunity. Chen et al. developed a putaminal nanocomplex (BTO-Pd-MnO_2-HA NPs) to enhance BTO-mediated SDT by incorporating CDT [104]. The synthesis involved sequentially loading palladium nanoparticles onto BTO, coating them with MnO_2 to form BTO-Pd-MnO_2 NPs, and finally modifying the surface with hyaluronic acid (HA). In melanoma treatment, HA facilitates tumor targeting, allowing nanoparticle accumulation. MnO_2 reacts with TME-derived H_2O_2 to generate O_2 and Mn^{2+} while depleting glutathione, increasing ROS sensitivity. Mn^{2+} further contributes to •OH production via a Fenton-like reaction. Ultrasound stimulation induces Schottky junction formation between BTO and Pd, reducing electron-hole recombination. Elevated O_2 levels boost ROS generation, promoting tumor cell apoptosis. Results indicated increased expression of cleaved caspase-3 and Bax, reduced Bcl-2, and significant downregulation of HIF-1α. TUNEL staining revealed extensive DNA fragmentation, while

Ki67 immunohistochemistry confirmed suppressed cell proliferation, validating the efficacy of BTO-based SDT and CDT for tumor therapy.

6.3. Combined with Chemotherapy

Chemotherapy is a common cancer treatment but is often accompanied by severe side effects. Combining SDT with chemotherapy enhances antitumor effects through synergistic mechanisms while lowering drug dosage and minimizing adverse reactions. Upon ultrasound activation, SDT produces highly reactive ROS that induce tumor cell apoptosis and deplete antioxidants like GSH, increasing the sensitivity of cancer cells to chemotherapy [105]. Additionally, SDT mitigates tumor hypoxia, making chemotherapy more effective against hypoxic tumors. Ultrasound stimulation further improves drug penetration and targeted delivery [106]. This dual therapy not only amplifies anticancer efficacy but also reduces systemic toxicity, improving patient tolerance and offering a safer treatment strategy.

A simple approach involves co-delivering chemotherapeutic agents with a piezocatalyst [54,107]. For example, Hoang et al. constructed piperlongumine (PL)-loaded, Au-decorated zinc oxide nanorods (PL-Au@P-ZnO NRs) [54]. Like other hybrid piezocatalysts, Au@ZnO enhances oxidative stress due to its remarkable piezoelectric properties and Fenton catalytic reactivity when exposed to ultrasound irradiation. The addition of the pro-oxidant PL further intensifies intracellular oxidative stress, leading to cancer-specific cytotoxicity. Gong et al. developed a dual-treatment strategy that combines low-dose chemotherapy with enhanced SDT, utilizing BTO nanoparticles as sonosensitizers for tumor organoid treatment [106]. Ultrasound increases the cellular uptake of chemotherapy drugs, while chemotherapy aids BTO's entry into tumor cells, resulting in a synergistic inhibition of tumor cell viability. This approach achieved efficacy similar to high-dose chemotherapy, significantly reducing drug dosage and side effects.

The piezoelectric effect, with its ability to convert electrical energy to mechanical energy, improves drug permeation in chemotherapy delivery systems. This enhancement is due to localized changes in the microenvironment, such as hydrodynamic effects and cell membrane potential modulation, which promote drug transport across membranes. SDT further facilitates controlled drug release, especially under ultrasound excitation, while also reducing chemotherapy drug dosage. The combination of these two therapies leads to a synergistic effect, enhancing efficacy and minimizing toxicity.

7. Biosafety and Biocompatibility of Piezoelectric Sonosensitizers

In biomedical applications, ensuring the biocompatibility and biosafety of sonosensitizers is essential, as these factors directly influence their clinical acceptance, therapeutic effectiveness, and safety. Evaluating these properties primarily involves two key aspects: hematological and tissue-specific assessments [108]. Hematological analysis includes blood biochemical markers (liver and kidney function), complete blood count (cell types, morphology, ratios, and total counts), and hemolysis tests, which collectively determine a material's compatibility with the circulatory system. Meanwhile, tissue-specific assessments focus on cytotoxicity, body weight fluctuations, and pathological changes in major organs, offering insights into the overall biosafety and tissue compatibility of the material. Extensive studies indicate that many piezoelectric materials demonstrate good biocompatibility and minimal toxicity in both in vitro and in vivo experiments, supporting their potential for clinical applications. The following sections summarize various strategies for improving biocompatibility and ensuring safety.

7.1. Surface Coating

Surface modification is a key strategy for improving both the biocompatibility and functionality of piezoelectric materials. By applying one or more layers of biocompatible substances—such as polymers, inorganic nanoparticles, or proteins—to their surface [109,110], crucial interfacial characteristics, including hydrophilicity, charge distribution, and biological recognition, can be optimized. This modification not only minimizes unintended interactions with biological systems, reducing immune rejection, but also introduces additional functional attributes, such as enhanced targeting and improved cell adhesion and differentiation. Additionally, surface coatings act as a protective barrier, shielding piezoelectric materials from rapid degradation caused by environmental factors like enzymatic activity and body fluid exposure.

Effective surface engineering strategies typically involve [110,111]: (1) covalent attachment of biocompatible polymers (e.g., polyethylene glycol, polyvinylpyrrolidone) to increase hydrophilicity and minimize nonspecific protein adsorption; (2) biomimetic functionalization with targeting ligands (e.g., RGD peptides, folic acid) to enhance tumor accumulation while reducing off-target effects; and (3) charge modulation via carboxylation or amination to influence cellular uptake and mitigate electrostatic-induced cytotoxicity. Advanced approaches incorporate hybrid coatings that integrate zwitterionic polymers with stimuli-responsive linkers, enabling "stealth" properties during systemic circulation while facilitating charge reversal at tumor sites. Furthermore, encapsulating piezoelectric cores within biodegradable silica or phospholipid bilayers effectively limits ionic leaching and allows for controlled degradation kinetics.

For instance, He et al. developed a semiconductor material with a wide bandgap, ytterbium-doped bismuth fluoride (BiF_3@Yb), surface-loaded with zinc phthalocyanine (ZnPc) and coated with an amphiphilic PEG layer. The resulting composite catalyst (BZP) exhibited excellent biocompatibility, effectively reducing immune responses in vivo and extending circulation time [112].

7.2. Enhancing Targeting

Enhancing the targeting ability of piezoelectric materials is a key approach in biomedical applications, aiming to improve treatment precision, efficacy, and safety [113]. By incorporating specific recognition features, such as surface functionalization with targeting ligands, these materials can selectively interact with designated cells or tissues. This targeted approach not only increases the specificity of SDT for diseased regions but also minimizes unintended damage to surrounding healthy tissues. Furthermore, integrating advanced imaging modalities—such as MRI, CT, and ultrasound imaging—enables real-time localization and monitoring of the therapeutic process, supporting the advancement of personalized medicine.

For example, Qian et al. coated BT nanoparticles with macrophage membranes that have been pre-activated by Staphylococcus aureus (MMSa) [114]. This nanoparticle delivery system (BTO@MMSa) took advantage of the higher expression of Toll-like receptors (TLRs) on MMSa-coated macrophage membranes compared to normal macrophage membranes. These MMSa-coated nanoparticles showed improved recognition and binding to bacteria, making them particularly useful for targeting bacterial infections in wounds and facilitating healing. In another study by Tang et al., BT nanoparticles were coated with macrophage membranes activated by matrix metalloproteinase 2 (MMP2) [15]. The MMP2-responsive macrophage membranes also incorporated PD-L1 blockade mechanisms (M@BTO NPs), enabling a dual-modality therapeutic approach. When exposed to US irradiation, the M@BTO NPs generated ROS to induce tumor cell death, while simultaneously producing oxygen to alleviate tumor hypoxia, thereby fostering an environment conducive to an enhanced

antitumor immune response. This combined effect promoted increased infiltration of CTLs and improved the efficacy of PD-L1 blockade therapy. By combining the piezocatalytic properties of BT-based sonosensitizers with the targeting and immunomodulatory capabilities of cell membranes, these advanced nanosystems offer a promising platform for precise and effective cancer treatment.

7.3. Degradability

Ideal biomedical materials should possess controllable degradation characteristics, ensuring they can be safely metabolized or excreted after completing their therapeutic role. For piezoelectric materials, improving degradability requires tailoring their chemical composition and structural properties to enable gradual breakdown within the physiological environment while preserving their sonodynamic functionality. This approach not only mitigates potential biosafety concerns associated with prolonged material retention but also reduces the foreign body burden on patients. However, when these materials are exposed to ultrasound, especially at nanometric scales, they may undergo accelerated degradation due to the mechanical forces generated by cavitation and other acoustic effects. The degradation products of piezoelectric materials, such as metal ions or fragments, could potentially induce toxicity, posing additional challenges to their clinical application. Therefore, it is crucial to evaluate the biodegradability of these materials under ultrasound exposure and to assess whether their degradation by-products might lead to adverse biological effects, such as inflammation or neurotoxicity [68,69]. Strategies for enhancing degradation typically include surface modifications, incorporation of biodegradable components, and fine-tuning of material microstructures. For instance, Chen et al. designed a biodegradable three-dimensional piezoelectric scaffold composed of poly(lactic acid) nanofibers and sodium potassium niobate nanowires, which demonstrated effective spinal cord injury repair in rats while progressively degrading post-treatment, thereby minimizing long-term foreign body accumulation [115].

8. Summary and Outlook

As a novel, non-invasive therapeutic modality, SDT boasts numerous advantages, including minimal invasiveness, reduced trauma, high selectivity, precision, safety, repeatability, and the capacity to target deeply embedded tissues. These attributes render SDT a promising complement, or even an alternative, to conventional cancer therapies, offering safer and more effective treatment options for patients. This review offers a comprehensive analysis of the pivotal role and prospective applications of piezoelectric materials in SDT, with a particular emphasis on their utilization in cancer treatment. By harnessing their unique piezoelectric characteristics, these materials significantly enhance the generation of ROS under US stimulation, thereby exerting potent cytotoxic effects on tumor cells.

In SDT, piezoelectric materials serve as critical sonosensitizers. Upon exposure to ultrasonic mechanical stress, these materials generate internal electric fields that drive redox reactions, thereby facilitating ROS production and directly triggering apoptosis or necrosis in tumor cells. Notably, inorganic piezoelectric materials such as barium titanate, molybdenum disulfide, zinc oxide, and bismuth-based compounds exhibit outstanding performance in SDT due to their superior chemical stability, physical resilience, and higher piezoelectric coefficients.

Furthermore, cancer sonodynamic immunotherapy represents an innovative therapeutic approach that synergistically combines sonosensitizers with immuno-oncological agents to activate potent antitumor immune responses. Sonosensitizers generate ROS under US irradiation, inducing tumor cell death and promoting ICD to enhance tumor immunogenicity. Simultaneously, immuno-oncology drugs modulate diverse immune pathways

to elicit robust immune responses. With its exceptional tissue penetration, precise spatial and temporal control, and the synergistic effects of sonosensitizers and immunotherapy, sono-immunotherapy holds immense promise for safely and effectively treating deeply located malignancies. This review also consolidates recent advancements in integrating piezoelectric sonosensitizer-based SDT with various immunotherapeutic strategies, showcasing their great potential as innovative, integrated cancer therapies capable of boosting antitumor immunity and overcoming the limitations of traditional immunotherapy and SDT.

Despite considerable advancements and promising results, many piezoelectric-based sonodynamic systems remain in the proof-of-concept stage. Several key challenges must be addressed before these therapies can be translated into clinical practice, including:

1. Enhancing the physicochemical properties and targeting efficiency of sonosensitizers through surface modifications is crucial. These modifications can help minimize uptake by the reticuloendothelial system, extend the circulation time in the bloodstream, and improve the accumulation of the agents at diseased sites. However, surface engineering techniques are still in the early stages of development, requiring further research to optimize their effectiveness. Furthermore, the incorporation of functional compounds onto sonosensitizer surfaces raises concerns about potential toxicity, necessitating thorough evaluation and optimization for clinical application.
2. Another critical consideration is whether nanoparticles degrade under ultrasound exposure, as this could significantly influence their safety profile. Under ultrasound stimulation, some nanomaterials may undergo degradation, potentially releasing harmful byproducts into the body. These degradation products, depending on the material composition, could pose cytotoxic risks or lead to unwanted biological interactions. For instance, certain metal oxide nanoparticles may release metal ions upon ultrasound-induced breakdown, which could cause oxidative stress, inflammation, or organ toxicity. Thus, understanding the degradation behavior of nanoparticles under therapeutic ultrasound and evaluating the toxicity of their degradation products are essential steps to ensure the safe application of sonosensitizers in clinical settings.
3. While SDT is primarily associated with cavitation and ROS generation, the dominant mechanisms and potential synergistic effects remain poorly understood. The complexity of intracellular and in vivo environments complicates the assessment of these processes, making it difficult to evaluate their effects with current methodologies. Innovative approaches to studying these mechanisms are critical to advancing SDT strategies, informing the design of next-generation sonosensitizers, and enabling their clinical translation.
4. The efficacy of SDT heavily depends on the development of optimized sonosensitizers. While inorganic sonosensitizers have demonstrated clinical promise, issues such as low sonodynamic efficiency, limited biocompatibility, adverse side effects, poor solubility, and insufficient tumor targeting need to be addressed to facilitate clinical adoption. Continued research is required to resolve these challenges and enhance the performance of sonosensitizers.
5. The physical properties of ultrasound, including intensity and pulse frequency, significantly affect the efficacy of SDT. For example, the formation of standing waves from ultrasonic wave interference can amplify therapeutic effects at tumor sites. Optimizing ultrasound equipment and parameters could enhance SDT-based immunotherapy outcomes. Additionally, as ultrasound-based nanomedicines grow more complex, integrating multiple components to improve SDT efficiency and overcome TME limitations presents manufacturing challenges. The development of scalable, standardized

synthesis methods will be crucial to ensuring reproducibility and facilitating the clinical adoption of these therapies.

In conclusion, piezoelectric materials offer substantial promise in advancing SDT as a cutting-edge cancer treatment. With continued research and technological innovation, SDT is gaining recognition for its non-invasive nature, therapeutic efficacy, and potential for personalized medicine. As the field progresses, SDT is poised to become an integral component of modern cancer therapies, offering new hope for effective and targeted treatments.

Author Contributions: Conceptualization, G.W. and Z.L.; writing—original draft preparation, G.W. and Y.Q.; writing—review and editing, G.W. and Z.L.; supervision, R.W.; funding acquisition, R.W. All authors have read and agreed to the published version of the manuscript.

Funding: This research was funded by Shandong Provincial Natural Science Foundation, grant number ZR2024QF165.

Data Availability Statement: No new data were created or analyzed in this study.

Conflicts of Interest: The authors declare no conflicts of interest.

References

1. Mitragotri, S. Healing sound: The use of ultrasound in drug delivery and other therapeutic applications. *Nat. Rev. Drug Discov.* **2005**, *4*, 255–260. [PubMed]
2. Mallidi, S.; Anbil, S.; Bulin, A.-L.; Obaid, G.; Ichikawa, M.; Hasan, T. Beyond the barriers of light penetration: Strategies, perspectives and possibilities for photodynamic therapy. *Theranostics* **2016**, *6*, 2458.
3. Yang, K.; Zhao, S.; Li, B.; Wang, B.; Lan, M.; Song, X. Low temperature photothermal therapy: Advances and perspectives. *Coord. Chem. Rev.* **2022**, *454*, 214330.
4. Pan, J.; Xu, Y.; Wu, Q.; Hu, P.; Shi, J. Mild magnetic hyperthermia-activated innate immunity for liver cancer therapy. *J. Am. Chem. Soc.* **2021**, *143*, 8116–8128.
5. De Ruysscher, D.; Niedermann, G.; Burnet, N.G.; Siva, S.; Lee, A.W.; Hegi-Johnson, F. Radiotherapy toxicity. *Nat. Rev. Dis. Primers* **2019**, *5*, 13.
6. Zhang, Y.; Zhang, X.; Yang, H.; Yu, L.; Xu, Y.; Sharma, A.; Yin, P.; Li, X.; Kim, J.S.; Sun, Y. Advanced biotechnology-assisted precise sonodynamic therapy. *Chem. Soc. Rev.* **2021**, *50*, 11227–11248. [PubMed]
7. Zhang, C.; Pu, K. Organic sonodynamic materials for combination cancer immunotherapy. *Adv. Mater.* **2023**, *35*, 2303059.
8. Ivanova, V.A.; Verenikina, E.V.; Nikitina, V.P.; Zhenilo, O.E.; Ardzha, A.Y. Photodynamic therapy for preinvasive vaginal cancer. *J. Clin. Oncol.* **2021**, *39* (Suppl. 15), 5592.
9. Wan, Y.; Fu, L.H.; Li, C.; Lin, J.; Huang, P. Conquering the hypoxia limitation for photodynamic therapy. *Adv. Mater.* **2021**, *33*, 2103978.
10. Koruza, J.; Bell, A.J.; Frmling, T.; Webber, K.G.; Wang, K.; Rdel, J. Requirements for the transfer of lead-free piezoceramics into application. *J. Mater.* **2018**, *4*, 13–26.
11. Xing, J.; Chen, H.; Jiang, L.; Zhao, C.; Tan, Z.; Huang, Y.; Wu, B.; Chen, Q.; Xiao, D.; Zhu, J. High performance $BiFe_{0.9}Co_{0.1}O_3$ doped KNN-based lead-free ceramics for acoustic energy harvesting. *Nano Energy* **2021**, *84*, 105900.
12. Su, R.; Wang, Z.; Zhu, L.; Pan, Y.; Zhang, D.; Wen, H.; Luo, Z.D.; Li, L.; Li, F.T.; Wu, M.; et al. Strain-Engineered Nano-Ferroelectrics for High-Efficiency Piezocatalytic Overall Water Splitting. *Angew. Chem. Int. Ed. Engl.* **2021**, *60*, 16019–16026.
13. Wang, K.; Han, C.; Li, J.; Qiu, J.; Sunarso, J.; Liu, S. The mechanism of piezocatalysis: Energy band theory or screening charge effect? *Angew. Chem. Int. Ed. Engl.* **2022**, *134*, e202110429.
14. Starr, M.B.; Wang, X. Coupling of piezoelectric effect with electrochemical processes. *Nano Energy* **2015**, *14*, 296–311.
15. Tang, Q.; Sun, S.; Wang, P.; Sun, L.; Wang, Y.; Zhang, L.; Xu, M.; Chen, J.; Wu, R.; Zhang, J. Genetically engineering cell membrane-coated BTO nanoparticles for MMP2-activated piezocatalysis-immunotherapy. *Adv. Mater.* **2023**, *35*, 2300964.
16. Zhao, Y.; Wang, S.; Yao, S.; Wan, X.; Hu, Q.; Zheng, M.; Wang, Z.; Li, L. Piezoelectric $Ba_{0.85}Sr_{0.15}TiO_3$ Nanosonosensitizer with Nitric Oxide Delivery for Boosting Cancer Therapy. *Small Methods* **2024**, *8*, 2301134.
17. Cai, L.; Sun, T.; Han, F.; Zhang, H.; Zhao, J.; Hu, Q.; Shi, T.; Zhou, X.; Cheng, F.; Peng, C. Degradable and Piezoelectric Hollow ZnO Heterostructures for Sonodynamic Therapy and Pro-Death Autophagy. *J. Am. Chem. Soc.* **2024**, *146*, 34188–34198.

18. Ma, Y.; Cao, Y.; Zu, M.; Gao, Q.; Liu, G.; Ji, J.; Xu, H.; Yang, Q.; Shi, X.; Reis, R.L. Flying-Saucer-Shaped Nanoheterojunctions with Enhanced Colorectal Tumor Accumulation for Increased Oxidative Stress and Immunometabolic Regulation. *Adv. Funct. Mater.* **2024**, *34*, 2402164.
19. Pu, Y.; Zhou, B.; Bing, J.; Wang, L.; Chen, M.; Shen, Y.; Gao, S.; Zhou, M.; Wu, W.; Shi, J. Ultrasound-triggered and glycosylation inhibition-enhanced tumor piezocatalytic immunotherapy. *Nat. Commun.* **2024**, *15*, 9023. [PubMed]
20. Lv, S.; Qiu, Z.; Yu, D.; Wu, X.; Yan, X.; Ren, Y.; Huang, Y.; Jiang, G.; Gao, F. Custom-Made Piezoelectric Solid Solution Material for Cancer Therapy. *Small* **2023**, *19*, 2300976.
21. Kapat, K.; Shubhra, Q.T.; Zhou, M.; Leeuwenburgh, S. Piezoelectric nano-biomaterials for biomedicine and tissue regeneration. *Adv. Funct. Mater.* **2020**, *30*, 1909045. [CrossRef]
22. Khokhlova, V.A.; Fowlkes, J.B.; Roberts, W.W.; Schade, G.R.; Xu, Z.; Khokhlova, T.D.; Hall, T.L.; Maxwell, A.D.; Wang, Y.-N.; Cain, C.A. Histotripsy methods in mechanical disintegration of tissue: Towards clinical applications. *Int. J. Hyperther.* **2015**, *31*, 145–162. [CrossRef]
23. Copelan, A.; Hartman, J.; Chehab, M.; Venkatesan, A.M. *High-Intensity Focused Ultrasound: Current Status for Image-Guided Therapy*; Seminars in Interventional Radiology; Thieme Medical Publishers: New York, NY, USA, 2015; pp. 398–415.
24. Watanabe, Y.; Aoi, A.; Horie, S.; Tomita, N.; Mori, S.; Morikawa, H.; Matsumura, Y.; Vassaux, G.; Kodama, T. Low-intensity ultrasound and microbubbles enhance the antitumor effect of cisplatin. *Cancer Sci.* **2008**, *99*, 2525–2531. [CrossRef]
25. Ranvier, G.G.F.; Shouhed, D.; Inabnet, W.B. Minimally invasive techniques for resection of pancreatic neuroendocrine tumors. *Surg. Oncol. Clin.* **2016**, *25*, 195–215. [CrossRef]
26. McHale, A.P.; Callan, J.F.; Nomikou, N.; Fowley, C.; Callan, B. Sonodynamic therapy: Concept, mechanism and application to cancer treatment. *Ther. Ultrasound* **2016**, *880*, 429–450.
27. Umemura, S.I.; Yumita, N.; Nishigaki, R.; Umemura, K. Mechanism of cell damage by ultrasound in combination with hematoporphyrin. *Jpn. J. Cancer Res.* **1990**, *81*, 962–966. [CrossRef] [PubMed]
28. Ivanova, V.A.; Verenikina, E.V.; Nikitina, V.P.; Zhenilo, O.E.; Kruze, P.A.; Nikitin, I.S.; Kit, O.I. Photodynamic therapy for preinvasive cervical cancer. *J. Clin. Oncol.* **2020**, *38*, 6035. [CrossRef]
29. Gong, F.; Cheng, L.; Yang, N.; Betzer, O.; Feng, L.; Zhou, Q.; Li, Y.; Chen, R.; Popovtzer, R.; Liu, Z. Ultrasmall oxygen-deficient bimetallic oxide $MnWO_X$ nanoparticles for depletion of endogenous GSH and enhanced sonodynamic cancer therapy. *Adv. Mater.* **2019**, *31*, 1900730. [CrossRef]
30. Wang, X.; Zhong, X.; Bai, L.; Xu, J.; Gong, F.; Dong, Z.; Yang, Z.; Zeng, Z.; Liu, Z.; Cheng, L. Ultrafine titanium monoxide (TiO_{1+x}) nanorods for enhanced sonodynamic therapy. *ACS Nano* **2020**, *142*, 6527–6537. [CrossRef]
31. Zhu, P.; Chen, Y.; Shi, J. Nanoenzyme-augmented cancer sonodynamic therapy by catalytic tumor oxygenation. *ACS Nano* **2018**, *12*, 3780–3795. [CrossRef] [PubMed]
32. Liang, S.; Deng, X.; Ma, P.A.; Cheng, Z.; Lin, J. Recent Advances in Nanomaterial-Assisted Combinational Sonodynamic Cancer Therapy. *Adv. Mater.* **2020**, *32*, 2003214. [CrossRef]
33. Wan, G.-Y.; Liu, Y.; Chen, B.-W.; Liu, Y.-Y.; Wang, Y.-S.; Zhang, N. Recent advances of sonodynamic therapy in cancer treatment. *Cancer Biol. Med.* **2016**, *13*, 325. [CrossRef] [PubMed]
34. Canavese, G.; Ancona, A.; Racca, L.; Canta, M.; Dumontel, B.; Barbaresco, F.; Limongi, T.; Cauda, V. Nanoparticle-assisted ultrasound: A special focus on sonodynamic therapy against cancer. *Chem. Eng. J.* **2018**, *340*, 155–172. [CrossRef] [PubMed]
35. Choi, V.; Rajora, M.A.; Zheng, G. Activating drugs with sound: Mechanisms behind sonodynamic therapy and the role of nanomedicine. *Bioconjug. Chem.* **2020**, *31*, 967–989. [CrossRef] [PubMed]
36. Zheng, H.; Lin, H.; Tian, H.; Lin, K.; Yang, F.; Zhang, X.; Ge, S.; Fan, X.; Jia, R.; Ruan, J. Steering Piezocatalytic Therapy for Optimized Tumoricidal Effect. *Adv. Funct. Mater.* **2024**, *34*, 2400174. [CrossRef]
37. Li, F.; Zhang, S.; Yang, T.; Xu, Z.; Zhang, N.; Liu, G.; Wang, J.; Wang, J.; Cheng, Z.; Ye, Z.-G. The origin of ultrahigh piezoelectricity in relaxor-ferroelectric solid solution crystals. *Nat. Commun.* **2016**, *7*, 13807. [CrossRef]
38. Zheng, T.; Wu, J.; Xiao, D.; Zhu, J. Recent development in lead-free perovskite piezoelectric bulk materials. *Prog. Mater. Sci.* **2018**, *98*, 552–624.
39. Zhou, X.; Shen, B.; Lyubartsev, A.; Zhai, J.; Hedin, N. Semiconducting piezoelectric heterostructures for piezo-and piezophotocatalysis. *Nano Energy* **2022**, *96*, 107141. [CrossRef]
40. Hong, K.-S.; Xu, H.; Konishi, H.; Li, X. Direct water splitting through vibrating piezoelectric microfibers in water. *J. Phys. Chem. Lett.* **2010**, *1*, 997–1002. [CrossRef]
41. Wang, K.; Han, C.; Shao, Z.; Qiu, J.; Wang, S.; Liu, S. Perovskite oxide catalysts for advanced oxidation reactions. *Adv. Funct. Mater.* **2021**, *31*, 2102089. [CrossRef]
42. Tian, W.; Qiu, J.; Li, N.; Chen, D.; Xu, Q.; Li, H.; He, J.; Lu, J. Efficient piezocatalytic removal of BPA and Cr (VI) with SnS_2/CNFs membrane by harvesting vibration energy. *Nano Energy* **2021**, *86*, 106036.

43. Li, S.; Zhao, Z.; Yu, D.; Zhao, J.-Z.; Su, Y.; Liu, Y.; Lin, Y.; Liu, W.; Xu, H.; Zhang, Z. Few-layer transition metal dichalcogenides (MoS_2, WS_2, and WSe_2) for water splitting and degradation of organic pollutants: Understanding the piezocatalytic effect. *Nano Energy* **2019**, *66*, 104083.
44. Zhang, A.; Liu, Z.; Xie, B.; Lu, J.; Guo, K.; Ke, S.; Shu, L.; Fan, H. Vibration catalysis of eco-friendly $Na_{0.5}K_{0.5}NbO_3$-based piezoelectric: An efficient phase boundary catalyst. *Appl. Catal. B* **2020**, *279*, 119353. [CrossRef]
45. Wu, J.; Xu, Q.; Lin, E.; Yuan, B.; Qin, N.; Thatikonda, S.K.; Bao, D. Insights into the role of ferroelectric polarization in piezocatalysis of nanocrystalline $BaTiO_3$. *ACS Appl. Mater. Interfaces* **2018**, *10*, 17842–17849.
46. Shi, J.; Zeng, W.; Dai, Z.; Wang, L.; Wang, Q.; Lin, S.; Xiong, Y.; Yang, S.; Shang, S.; Chen, W. Piezocatalytic foam for highly efficient degradation of aqueous organics. *Small Sci.* **2021**, *1*, 2000011.
47. Wei, Y.; Zhang, Y.; Geng, W.; Su, H.; Long, M. Efficient bifunctional piezocatalysis of $Au/BiVO_4$ for simultaneous removal of 4-chlorophenol and Cr (VI) in water. *Appl. Catal. B* **2019**, *259*, 118084.
48. Shi, J.; Starr, M.B.; Wang, X. Band structure engineering at heterojunction interfaces via the piezotronic effect. *Adv. Mater.* **2012**, *24*, 4683–4691.
49. Zhu, P.; Chen, Y.; Shi, J. Piezocatalytic tumor therapy by ultrasound-triggered and $BaTiO_3$-mediated piezoelectricity. *Adv. Mater.* **2020**, *32*, 2001976.
50. Wang, Y.; Xu, Y.; Dong, S.; Wang, P.; Chen, W.; Lu, Z.; Ye, D.; Pan, B.; Wu, D.; Vecitis, C.D. Ultrasonic activation of inert poly (tetrafluoroethylene) enables piezocatalytic generation of reactive oxygen species. *Nat. Commun.* **2021**, *12*, 3508. [PubMed]
51. Wang, Y.; Wen, X.; Jia, Y.; Huang, M.; Wang, F.; Zhang, X.; Bai, Y.; Yuan, G.; Wang, Y. Piezo-catalysis for nondestructive tooth whitening. *Nat. Commun.* **2020**, *11*, 1328. [PubMed]
52. Wu, J.; Wang, W.; Tian, Y.; Song, C.; Qiu, H.; Xue, H. Piezotronic effect boosted photocatalytic performance of heterostructured $BaTiO_3/TiO_2$ nanofibers for degradation of organic pollutants. *Nano Energy* **2020**, *77*, 105122. [CrossRef]
53. Ma, K.; Qi, G.; Wang, B.; Yu, T.; Zhang, Y.; Li, H.; Kitte, S.A.; Jin, Y. Ultrasound-activated Au/ZnO-based Trojan nanogenerators for combined targeted electro-stimulation and enhanced catalytic therapy of tumor. *Nano Energy* **2021**, *87*, 106208.
54. Hoang, Q.T.; Ravichandran, V.; Cao, T.G.N.; Kang, J.H.; Ko, Y.T.; Lee, T.I.; Shim, M.S. Piezoelectric Au-decorated ZnO nanorods: Ultrasound-triggered generation of ROS for piezocatalytic cancer therapy. *Chem. Eng. J.* **2022**, *435*, 135039. [CrossRef]
55. Ma, W.; Lu, J.; Wan, B.; Peng, D.; Xu, Q.; Hu, G.; Peng, Y.; Pan, C.; Wang, Z.L. Piezoelectricity in multilayer black phosphorus for piezotronics and nanogenerators. *Adv. Mater.* **2020**, *32*, 1905795. [CrossRef] [PubMed]
56. Tan, D.; Willatzen, M.; Wang, Z.L. Prediction of strong piezoelectricity in 3R-MoS_2 multilayer structures. *Nano Energy* **2019**, *56*, 512–515. [CrossRef]
57. Wang, H.; Li, Z.; Shi, S.; Fan, X.; Sun, Z.; Liu, J.; Li, P.; Zhai, J.; Pan, Z. Harnessing piezoelectric and flexoelectric synergies in one-dimensional heterostructure nanofibers for nano-energy harvesting and self-powered sensors. *Chem. Eng. J.* **2023**, *474*, 145470. [CrossRef]
58. Yang, F.; Li, J.; Long, Y.; Zhang, Z.; Wang, L.; Sui, J.; Dong, Y.; Wang, Y.; Taylor, R.; Ni, D. Wafer-scale heterostructured piezoelectric bio-organic thin films. *Science* **2021**, *373*, 337–342. [CrossRef]
59. Zhao, C.; Huang, Y.; Wu, J. Multifunctional barium titanate ceramics via chemical modification tuning phase structure. *InfoMat* **2020**, *2*, 1163–1190. [CrossRef]
60. Zhao, Y.; Wang, S.; Ding, Y.; Zhang, Z.; Huang, T.; Zhang, Y.; Wan, X.; Wang, Z.L.; Li, L. Piezotronic Effect-Augmented $Cu_{2-x}O$–$BaTiO_3$ Sonosensitizers for Multifunctional Cancer Dynamic Therapy. *ACS Nano* **2022**, *16*, 9304–9316. [CrossRef]
61. Wang, L.; Zhang, X.; You, Z.; Yang, Z.; Guo, M.; Guo, J.; Liu, H.; Zhang, X.; Wang, Z.; Wang, A. A Molybdenum Disulfide Nanozyme with Charge-Enhanced Activity for Ultrasound-Mediated Cascade-Catalytic Tumor Ferroptosis. *Angew. Chem. Int. Ed.* **2023**, *62*, e202217448. [CrossRef]
62. Du, Y.; Yang, J.; He, F.; Zhao, X.; Zhou, J.; Zang, P.; Liu, C.; Xie, Y.; Zhang, Y.; Yang, P. Revealing the mutually enhanced mechanism of necroptosis and immunotherapy induced by defect engineering and piezoelectric effect. *Adv. Mater.* **2024**, *36*, 2304322. [CrossRef]
63. Deng, R.; Zhou, H.; Qin, Q.; Ding, L.; Song, X.; Chang, M.; Chen, Y.; Zhou, Y. Palladium-Catalyzed Hydrogenation of Black Barium Titanate for Multienzyme-Piezoelectric Synergetic Tumor Therapy. *Adv. Mater.* **2024**, *36*, 2307568. [CrossRef]
64. Truong Hoang, Q.; Kim, D.Y.; Park, H.S.; Jang, W.; Nguyen Cao, T.G.; Kang, J.H.; Ko, Y.T.; Mun, S.J.; Bhang, S.H.; Shim, M.S. Oxygen-Supplying Piezocatalytic Therapy of Hypoxic Tumors by Intratumoral Delivery of pH-Responsive Multicompartmental Carriers with Sequential Drug Release Capability. *Adv. Funct. Mater.* **2024**, *34*, 2306078. [CrossRef]
65. Han, Q.; Fang, Z.; Lin, R.; Chen, J.; Wei, X.; Gong, C.; Yang, Z.; Zou, P.; Zhu, J.; Xing, L. Piezo-photodynamic therapy of Au@ PEG-ZnO nanostructures enabled with a battery-free wireless cancer therapeutic dot. *Nano Energy* **2024**, *125*, 109530. [CrossRef]
66. Ji, H.; Yu, K.; Wang, H.; Yang, H. Nanoclay Mediated Self-Promoted Reactive Oxygen Species Releasing Enables Efficient Antimicrobial. *Adv. Funct. Mater.* **2024**, *34*, 2407875. [CrossRef]
67. Tian, B.; Tian, R.; Liu, S.; Wang, Y.; Gai, S.; Xie, Y.; Yang, D.; He, F.; Yang, P.; Lin, J. Doping engineering to modulate lattice and electronic structure for enhanced piezocatalytic therapy and ferroptosis. *Adv. Mater.* **2023**, *35*, 2304262. [CrossRef]

68. Guo, Z.; Zhang, P.; Luo, Y.; Xie, H.Q.; Chakraborty, S.; Monikh, F.A.; Bu, L.; Liu, Y.; Ma, Y.; Zhang, Z. Intranasal exposure to ZnO nanoparticles induces alterations in cholinergic neurotransmission in rat brain. *Nano Today* **2020**, *35*, 100977. [CrossRef]
69. Zhang, Y.; Zhang, Y.; Lei, Y.; Wu, J.; Kang, Y.; Zheng, S.; Shao, L. MDM2 upregulation induces mitophagy deficiency via Mic60 ubiquitination in fetal microglial inflammation and consequently neuronal DNA damage caused by exposure to ZnO-NPs during pregnancy. *J. Hazard. Mater.* **2023**, *457*, 131750. [CrossRef]
70. Guo, Z.; Zhang, P.; Xie, H.Q.; Zhao, B.; Lynch, I. First in vivo evidence for compromised brain energy metabolism upon intranasal exposure to ZnO nanoparticles. *Environ. Sci. Technol. Lett.* **2020**, *7*, 315–322. [CrossRef]
71. Vopson, M.M. Fundamentals of multiferroic materials and their possible applications. *Crit. Rev. Solid State Mater. Sci.* **2015**, *40*, 223–250. [CrossRef]
72. Eerenstein, W.; Mathur, N.; Scott, J.F. Multiferroic and magnetoelectric materials. *Nature* **2006**, *442*, 759–765.
73. Yu, C.; Li, J.; Zang, P.; Feng, L.; Tian, B.; Zhao, R.; Xie, Y.; Wu, L.; Chen, Z.; Yang, P. A Functional "Key" Amplified Piezoelectric Effect Modulates ROS Storm with an Open Source for Multimodal Synergistic Cancer Therapy. *Small* **2024**, *20*, 2401931.
74. Bai, G.; Yuan, S.; Zhao, Y.; Yang, Z.; Choi, S.Y.; Chai, Y.; Yu, S.F.; Lau, S.P.; Hao, J. 2D layered materials of rare-earth Er-doped MoS_2 with NIR-to-NIR down-and up-conversion photoluminescence. *Adv. Mater.* **2016**, *28*, 7472–7477.
75. Wu, J.M.; Chang, W.E.; Chang, Y.T.; Chang, C.-K. Piezo-Catalytic Effect on the Enhancement of the Ultra-High Degradation Activity in the Dark by Single-and Few-Layers MoS2 Nanoflowers. *Adv. Mater.* **2016**, *28*, 3718–3725.
76. Xia, L.; Chen, J.; Xie, Y.; Zhang, S.; Xia, W.; Feng, W.; Chen, Y. Photo-/piezo-activated ultrathin molybdenum disulfide nanomedicine for synergistic tumor therapy. *J. Mater. Chem. B* **2023**, *11*, 2895–2903.
77. Wu, Q.; Zhang, J.; Pan, X.; Huang, Z.; Zhang, H.; Guo, J.; Xue, Y.; Shi, R.; Liu, H. Vacancy Augmented Piezo-Sonosensitizer for Cancer Therapy. *Adv. Sci.* **2023**, *10*, 2301152.
78. Mohan, R. Green bismuth. *Nat. Chem.* **2010**, *2*, 336. [PubMed]
79. Chen, G.; Li, Y.; Liu, B.; Miao, Y. Recent developments in bismuth oxyhalide-based functional nanomaterials for biomedical applications. *Biomater. Sci.* **2022**, *10*, 5809–5830. [CrossRef]
80. Wang, Q.; Du, J.; Ouyang, R.; Liu, B.; Miao, Y.; Li, Y. Recent advances in functional bismuth chalcogenide nanomaterials: Cancer theranostics, antibacterial and biosensing. *Coord. Chem. Rev.* **2023**, *492*, 215281.
81. Du, J.; He, Z.; Wang, Q.; Chen, G.; Li, X.; Lu, J.; Qi, Q.; Ouyang, R.; Miao, Y.; Li, Y. Topochemical-like bandgap regulation engineering: A bismuth thiooxide nanocatalyst for breast cancer phototherapy. *J. Colloid Interface Sci.* **2024**, *662*, 171–182. [CrossRef]
82. Wen, S.; Zhang, W.; Yang, J.; Zhou, Z.; Xiang, Q.; Dong, H. Ternary Bi_2WO_6/TiO_2–Pt Heterojunction Sonosensitizers for Boosting Sonodynamic Therapy. *ACS Nano* **2024**, *18*, 23672–23683. [CrossRef]
83. Cao, X.; Wang, Y.; Song, X.; Lou, W.; Li, X.; Lu, W.; Chen, K.; Chen, L.; Chen, Y.; Huang, B. Defect-Engineering Bismuth-Based Homologous Schottky Heterojunction for Metabolic Regulation-Augmented Sonodynamic Tumor Therapy. *Adv. Funct. Mater.* **2023**, *33*, 2300777.
84. Hu, G.; Wang, J.; Chen, L.; Zheng, H.; Lan, Y.; Wang, K.; Liu, X.; You, H.; Luo, Y.; Dong, L. Small-Bandgap Transducers Induced Carrier Separation for In Situ Dual-Amplified Tumor Oxidative Stress. *Adv. Funct. Mater.* **2024**, 2401897.
85. Wu, M.; Yong, J.; Zhang, H.; Wang, Z.; Xu, Z.P.; Zhang, R. 2D ultrathin iron doped bismuth oxychloride nanosheets with rich oxygen vacancies for enhanced sonodynamic therapy. *Adv. Healthc. Mater.* **2023**, *12*, 2301497.
86. Dong, Y.; Dong, S.; Liu, B.; Yu, C.; Liu, J.; Yang, D.; Yang, P.; Lin, J. 2D piezoelectric Bi_2MoO_6 nanoribbons for GSH-enhanced sonodynamic therapy. *Adv. Mater.* **2021**, *33*, 2106838.
87. Wang, J.; Zheng, H.; Hu, G.; Yang, X.; You, H.; Dong, L.; Song, S. Novel Spatially Asymmetric Copper Bismuthate-Mediated Augmentation of Energy Conversion to Realize "Three-Step" Tumor Suppression. *Adv. Sci.* **2024**, 2402599.
88. De Visser, K.E.; Joyce, J.A. The evolving tumor microenvironment: From cancer initiation to metastatic outgrowth. *Cancer Cell* **2023**, *41*, 374–403.
89. Mellman, I.; Chen, D.S.; Powles, T.; Turley, S.J. The cancer-immunity cycle: Indication, genotype, and immunotype. *Immunity* **2023**, *56*, 2188–2205. [PubMed]
90. Yong, T.; Wei, Z.; Gan, L.; Yang, X. Extracellular-vesicle-based drug delivery systems for enhanced antitumor therapies through modulating the cancer-immunity cycle. *Adv. Mater.* **2022**, *34*, 2201054.
91. Chen, D.S.; Mellman, I. Oncology meets immunology: The cancer-immunity cycle. *Immunity* **2013**, *39*, 1–10.
92. Liang, S.; Yao, J.; Liu, D.; Rao, L.; Chen, X.; Wang, Z. Harnessing nanomaterials for cancer sonodynamic immunotherapy. *Adv. Mater.* **2023**, *35*, 2211130. [CrossRef]
93. Yang, Y.; Huang, J.; Liu, M.; Qiu, Y.; Chen, Q.; Zhao, T.; Xiao, Z.; Yang, Y.; Jiang, Y.; Huang, Q. Emerging sonodynamic therapy-based nanomedicines for cancer immunotherapy. *Adv. Sci.* **2023**, *10*, 2204365. [CrossRef] [PubMed]
94. Wu, A.; Jiang, L.; Xia, C.; Xu, Q.; Zhou, B.; Jin, Z.; He, Q.; Guo, J. Ultrasound-Driven Piezoelectrocatalytic Immunoactivation of Deep Tumor. *Adv. Sci.* **2023**, *10*, 2303016. [CrossRef] [PubMed]

95. Wang, Q.; Du, J.; Yang, F.; Wu, S.; Zhu, L.; Li, X.; Yang, H.; Miao, Y.; Li, Y. Charge Separation-Engineered Piezoelectric Ultrathin Nanorods Modulate Tumor Stromal Microenvironment and Enhance Cell Immunogenicity for Synergistically Piezo-Thermal-Immune Therapy. *Small* **2024**, *21*, 2408038. [CrossRef]
96. Li, X.; Lovell, J.F.; Yoon, J.; Chen, X. Clinical development and potential of photothermal and photodynamic therapies for cancer. *Nat. Rev. Clin. Oncol.* **2020**, *17*, 657–674. [CrossRef]
97. Xiang, D.; Liu, Z.; Wu, M.; Liu, H.; Zhang, X.; Wang, Z.; Wang, Z.L.; Li, L. Enhanced piezo-photoelectric catalysis with oriented carrier migration in asymmetric Au− ZnO nanorod array. *Small* **2020**, *16*, 1907603. [CrossRef]
98. Wu, W.; Wang, Z.L. Piezotronics and piezo-phototronics for adaptive electronics and optoelectronics. *Nat. Rev. Mater.* **2016**, *1*, 16031. [CrossRef]
99. Dai, B.; Biesold, G.M.; Zhang, M.; Zou, H.; Ding, Y.; Wang, Z.L.; Lin, Z. Piezo-phototronic effect on photocatalysis, solar cells, photodetectors and light-emitting diodes. *Chem. Soc. Rev.* **2021**, *50*, 13646–13691. [CrossRef]
100. Cong, C.; Rao, C.; Ma, Z.; Yuan, Y.; Wang, D.; Zhang, X.; He, Y.; Lou, H.; Gao, D. Coupling piezo-photocatalysis to imitate lymphoid reflux for enhancing antitumor hydrodynamics therapy. *Chem. Eng. J.* **2022**, *450*, 137981. [CrossRef]
101. Zhang, R.; Yang, D.; Zang, P.; He, F.; Gai, S.; Kuang, Y.; Yang, G.; Yang, P. Structure Engineered High Piezo-Photoelectronic Performance for Boosted Sono-Photodynamic Therapy. *Adv. Mater.* **2024**, *36*, 2308355. [CrossRef] [PubMed]
102. Wu, J.; Meng, Y.; Wu, F.; Shi, J.; Sun, Q.; Jiang, X.; Liu, Y.; Zhao, P.; Wang, Q.; Guo, L. Ultrasound-Driven Non-Metallic Fenton-Active Center Construction for Extensive Chemodynamic Therapy. *Adv. Mater.* **2024**, *36*, 2307980. [CrossRef]
103. Wang, Y.; Tang, Q.; Wu, R.; Yang, S.; Geng, Z.; He, P.; Li, X.; Chen, Q.; Liang, X. Metformin-Mediated Fast Charge-Reversal Nanohybrid for Deep Penetration Piezocatalysis-Augmented Chemodynamic Immunotherapy of Cancer. *ACS Nano* **2024**, *18*, 6314–6332. [CrossRef] [PubMed]
104. Chen, C.; Yu, D.; Wang, W.; Huang, Y.; Ying, Y.; Sheng, W.; Wu, X.; Wang, Y.; Gao, F.; Jiang, G. Hyaluronic acid-covered piezoelectric nanocomposites as tumor microenvironment modulators for piezoelectric catalytic therapy of melanoma. *Int. J. Biol. Macromol.* **2023**, *236*, 124020. [CrossRef]
105. Zhang, T.; Zheng, Y.; Xiang, H.; Chen, Y.; Wu, R. Cascade piezocatalytic nanoprodrug for synergistic piezocatalytic therapy and sono-activated chemotherapy-augmented immunotherapy. *Nano Today* **2024**, *58*, 102453. [CrossRef]
106. Gong, Z.; Mao, Y.; Liu, Y.; Hu, X.; Zhang, Y.; Zhu, L.; Guo, S.; Ding, Z.; Zhang, L. Sono-promoted piezocatalysis and low-dose drug penetration for personalized therapy via tumor organoids. *J. Colloid Interface Sci.* **2024**, *675*, 192–206. [CrossRef]
107. He, Y.; Xu, Z.; He, Y.; Cao, G.; Ni, S.; Tang, Y.; Wang, J.; Yuan, Y.; Ma, Z.; Wang, D. MoS2 nanoflower-mediated enhanced intratumoral penetration and piezoelectric catalytic therapy. *Biomaterials* **2022**, *290*, 121816. [CrossRef] [PubMed]
108. Feliu, N.; Docter, D.; Heine, M.; Del Pino, P.; Ashraf, S.; Kolosnjaj-Tabi, J.; Macchiarini, P.; Nielsen, P.; Alloyeau, D.; Gazeau, F. In vivo degeneration and the fate of inorganic nanoparticles. *Chem. Soc. Rev.* **2016**, *45*, 2440–2457. [CrossRef]
109. Wei, W.; Zhang, X.; Chen, X.; Zhou, M.; Xu, R.; Zhang, X. Smart surface coating of drug nanoparticles with cross-linkable polyethylene glycol for bio-responsive and highly efficient drug delivery. *Nanoscale* **2016**, *8*, 8118–8125. [CrossRef] [PubMed]
110. Nam, J.; Won, N.; Bang, J.; Jin, H.; Park, J.; Jung, S.; Jung, S.; Park, Y.; Kim, S. Surface engineering of inorganic nanoparticles for imaging and therapy. *Adv. Drug Delivery Rev.* **2013**, *65*, 622–648. [CrossRef] [PubMed]
111. Karakoti, A.S.; Das, S.; Thevuthasan, S.; Seal, S. PEGylated inorganic nanoparticles. *Angew. Chem. Int. Ed.* **2011**, *50*, 1980–1994. [CrossRef]
112. He, Z.; Du, J.; Wang, Q.; Chen, G.; Li, X.; Zhang, Z.; Wang, S.; Jing, W.; Miao, Q.; Li, Y. Dye-augmented bandgap engineering of a degradable cascade nanoreactor for tumor immune microenvironment-enhanced dynamic phototherapy of breast cancer. *Acta Biomater.* **2024**, *176*, 390–404. [PubMed]
113. Dutta, B.; Barick, K.; Hassan, P. Recent advances in active targeting of nanomaterials for anticancer drug delivery. *Adv. Colloid Interface Sci.* **2021**, *296*, 102509. [CrossRef]
114. Qian, X.; Lu, T.; Huang, C.; Zheng, D.; Gong, G.; Chu, X.; Wang, X.; Lai, H.; Ma, L.; Jiang, L. Bioinspired Sonodynamic Nano Spray Accelerates Infected Wound Healing via Targeting and Disturbing Bacterial Metabolism. *Adv. Funct. Mater.* **2024**, *34*, 2315576. [CrossRef]
115. Chen, P.; Xu, C.; Wu, P.; Liu, K.; Chen, F.; Chen, Y.; Dai, H.; Luo, Z. Wirelessly powered electrical-stimulation based on biodegradable 3D piezoelectric scaffolds promotes the spinal cord injury repair. *ACS Nano* **2022**, *16*, 16513–16528. [PubMed]

Disclaimer/Publisher's Note: The statements, opinions and data contained in all publications are solely those of the individual author(s) and contributor(s) and not of MDPI and/or the editor(s). MDPI and/or the editor(s) disclaim responsibility for any injury to people or property resulting from any ideas, methods, instructions or products referred to in the content.